CHAPTER 19

Slope Stability

19.1 GENERAL

Slopes can be natural or manmade slopes (Figure 19.1). Natural slopes are found on the sides of mountains or at the edge of rivers, for example. Manmade slopes may be cut slopes, as in the case of an underpass for a road, or filled slopes, as in the case of an earth dam or a highway embankment. In all cases, the main parameter sought by the geotechnical engineer is the factor of safety against sliding failure of the slope.

Slopes fail along a failure surface. Most of the time, this surface can be approximated by a circle. However, the failure surface can take many other shapes, including a single plane, a series of planes, a log spiral, a sliding block, and others (Figure 19.2). Most analyses assume that the problem can be solved as if it were a plane strain problem in two dimensions. In three dimensions, the surface looks more like a spoon shape. Circular failure surfaces are the most common.

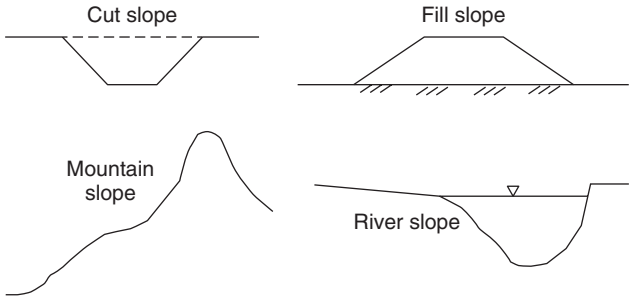

Figure 19.1 Natural slopes and manmade slopes.

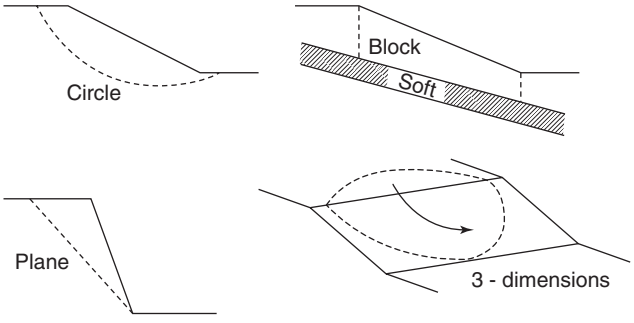

Figure 19.2 Failure surfaces.

19.2 DESIGN APPROACH

There are two aspects to slope stability: the safety against failure (ultimate limit state) and the movement under normal conditions (serviceability limit state). The movement under normal conditions is not often an issue and thus is rarely calculated; the best method for such estimates is the finite element method. The main issue is safety against failure; therefore, slope stability analysis consists of calculating the factor of safety F. Other issues include slope monitoring and slope stabilization methods. In the general case (circular failure surface), the factor of safety F is defined as (Figure 19.3):

$$F = \frac{\tau_{af}}{\tau_{am}} \tag{19.1}$$

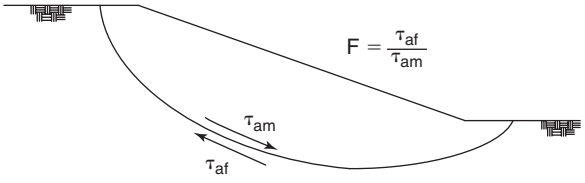

Figure 19.3 Factor of safety.

where τ_{af} is the average shear strength of the soil on the plane of failure and τ_{am} is the average shear stress mobilized on the plane of failure to keep the slope in equilibrium.

A simple example of how the factor of safety is obtained is shown in Figure 19.4. In this example the soil has a constant shear strength s along the length L of the failure plane, which is assumed to be an arc of a circle with a radius R and a center O. The weight of the failing soil mass is W, with a center of gravity generating a moment arm a around the center O. The factor of safety defined in Eq. 19.1 is also given in this

Geotechnical Engineering: Unsaturated and Saturated Soils Jean-Louis Briaud

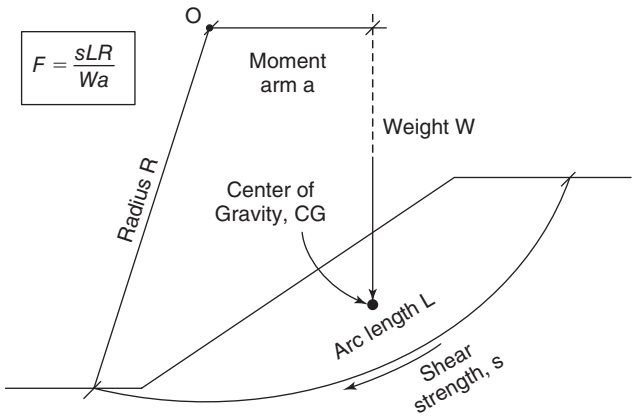

Figure 19.4 Simple slope stability problem.

case by the ratio of the maximum resisting moment over the driving moment around the center of the circle:

$$F = \frac{\tau_{af}}{\tau_{am}} = \frac{sLR}{Wa} \tag{19.2}$$

Note that because most of the time the slope stability problem is treated as a plane strain problem, the forces will be in kN/m and the moment in kN.m/m or kN. Typically the engineer will aim for a factor of safety between 1.25 and 1.5, depending on the application. As will be shown later, these values typically lead to a probability of failure that is higher than the probability of failure accepted in foundation engineering. Equation 19.2 is very simple; much more complexity is associated with slope stability analysis. The complexity arises from several issues:

1. The strength of the soil is not constant along the failure surface
2. The shape of the failure surface may vary (circle, plane, multilinear shape, log spiral)
3. One must find the failure surface corresponding to the lowest possible factor of safety
4. The boundary and external forces may be complex
5. The soil may be reinforced by inclusions

Equation 19.1 indicates how important it is to have a good estimate of the shear strength of the soil to obtain a good estimate of the factor of safety. The shear strength of soils was discussed in Chapter 15. The main equation is:

$$\tau_f = c' + (\sigma - \alpha u_w) \tan \varphi' \tag{19.3}$$

where τ_f is the shear strength, c' is the effective stress cohesion intercept, σ is the total normal stress on the failure plane, α is the area ratio coefficient for the water phase, u_w is the water stress, and φ' is the effective stress friction angle. The parameters c' and φ' can be obtained from a drained shear test (triaxial, direct shear, simple shear) or an undrained shear test with water stress measurements. The total stress σ can be calculated from the soil unit weight and any additional stress created by loading. The area ratio coefficient α can be estimated as the degree of saturation ($\alpha = S$) or through a correlation to the air entry value u_{wae} ($\alpha = (u_{wae}/u_w)^{0.5}$). If hydrostatic conditions exist, the water stress u_w can be estimated as follows. If the point considered is located under the groundwater level (GWL), u_w is the unit weight of water times the vertical distance from the point considered to the GWL. In this case the water stress is positive (compression). If the point considered is above the GWL in the zone that is saturated by capillary action, the water stress is also given as the unit weight of water times the distance between the point considered and the GWL, but this time the water stress is negative (tension). If the point considered is in the unsaturated zone above the zone saturated by capillary action, the water tension u_w can be estimated by its relationship with the water content through the soil water retention curve (SWRC). If the point considered is below the GWL but there is an excess water stress Δu_w, then the total water stress is the sum of the hydrostatic water stress and the excess water stress.

Because the factor of safety F involves the strength of the soil, it can be considered as an ultimate limit state where Eq. 19.1 is rewritten as:

$$\gamma \tau_{am} = \varphi \tau_{af} \tag{19.4}$$

where γ is the load factor and φ is the resistance factor. The values of γ and φ depend on how well the loading parameters and the shear strength parameters are known. The load factor in AASHTO (2007) for overall stability of slopes is taken as 1.0. The resistance factor φ proposed by AASHTO (2007) is:

- 0.75 if the geotechnical parameters are well defined and the slope does not support or contain a structural element
- 0.65 if the geotechnical parameters are not well defined or the slope supports or contains a structural element.

These resistance factors correspond to a probability of failure varying between 0.01 and 0.001.

19.3 INFINITE SLOPES

The simplest case of slope stability is the case where the slope is infinitely long (Figure 19.5). In this instance the

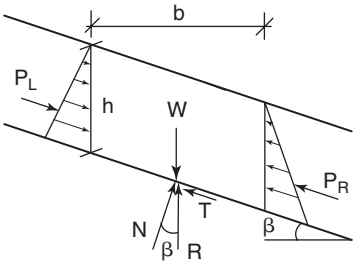

Figure 19.5 Infinite slope.

failure is assumed to be parallel to the ground surface. Several soil conditions, in order of increasing complexity, can be considered: dry sand, dry $c' - \varphi'$ soil, $c' - \varphi'$ soil with seepage, and $c' - \varphi'$ soil with unsaturated conditions.

19.3.1 Dry Sand

Consider a slice of the sheet of soil failing downslope. It is h high and b wide, and rests on the failure surface, which is at an angle β with the horizontal. The external forces acting on a free-body diagram of that slice include the weight of the slice W; the resistance R at the bottom of the slice, which can be decomposed into a normal force N and a shear force T; and the earth pressure force on the left P_L and the earth pressure force on the right P_R. The two forces P_L and P_R are equal, opposite, and in line with each other, so they simply cancel out of the equilibrium equation. The relationships between W, N, and T are:

$$N = W\cos\beta = \gamma bh\cos\beta \tag{19.5}$$

$$T = W\sin\beta = \gamma bh\sin\beta \tag{19.6}$$

where γ is the total unit weight of the dry sand. N and T represent the forces existing in the slope and mobilized to maintain the slope in equilibrium. The shear force S corresponding to the strength of the failure surface is not mobilized in the slope unless the slope is at failure. That force S represents the maximum value that T can have and is expressed as:

$$S = N\tan\varphi' = \gamma bh\cos\beta\tan\varphi' \tag{19.7}$$

The normal stress σ on the failure plane is:

$$\sigma = \frac{N}{A} = \frac{\gamma bh\cos\beta}{b/\cos\beta} = \gamma h\cos^2\beta \tag{19.8}$$

The shear stress τ on the plane of failure is:

$$\tau = \frac{T}{A} = \frac{\gamma bh\sin\beta}{b/\cos\beta} = \gamma h\sin\beta\cos\beta \tag{19.9}$$

The shear strength on the plane of failure is:

$$\tau_f = \frac{S}{A} = \frac{\gamma bh\cos\beta\tan\varphi'}{b/\cos\beta} = \gamma h\cos^2\beta\tan\varphi' \tag{19.10}$$

The factor of safety F is expressed as:

$$F = \frac{\tau_f}{\tau} = \frac{\gamma h\cos^2\beta\tan\varphi'}{\gamma h\sin\beta\cos\beta} = \frac{\tan\varphi'}{\tan\beta} \tag{19.11}$$

This is a very useful result, which says that a slope of dry sand cannot stand at an angle higher than the friction angle of the soil. This angle is usually around 30° for loose, dry sand. Next time you are at the beach, take a handful of dry sand, drop it gently on a flat surface, and measure the angle of the slope; this procedure will give you the friction angle of that loose sand, also called the *angle of repose*. Note that the factor of safety is independent of h, which means that all planes parallel to the ground surface are equally likely to be failure planes.

19.3.2 Dry $c' - \varphi'$ Soil

In the case of dry $c' - \varphi'$ soil, the only thing that changes is that the soil has a nonzero effective stress cohesion intercept c' in the expression of the shear strength (Eq. 19.10):

$$\tau_f = c' + \gamma h\cos^2\beta\tan\varphi' \tag{19.12}$$

Then the factor of safety becomes:

$$F = \frac{\tau_f}{\tau} = \frac{c' + \gamma h\cos^2\beta\tan\varphi'}{\gamma h\sin\beta\cos\beta} = \frac{c'}{\gamma h\sin\beta\cos\beta} + \frac{\tan\varphi'}{\tan\beta} \tag{19.13}$$

The factor of safety has increased compared to the dry sand case and depends on the depth h of the plane considered. Failure will occur on the plane defined by $F = 1$, called the *critical plane*, at a depth h_{crit}:

$$h_{cr} = \frac{c'}{\gamma\cos^2\beta(\tan\beta - \tan\varphi')} \tag{19.14}$$

Recall from section 15.16 that you can go from an effective stress solution to a total stress undrained solution by changing c' into s_u and taking φ' as equal to zero. Then the critical depth for the undrained case is.

$$h_{cr} = \frac{s_u}{\gamma\sin\beta\cos\beta} \tag{19.15}$$

19.3.3 $c' - \varphi'$ Soil with Seepage

In the case of $c' - \varphi'$ soil with seepage, the GWL is at the ground surface and the added complexity comes from having to take into account the influence of the water stress u_w on the shear strength. To obtain u_w, a flow net is drawn (Figure 19.6).

Recalling Eq. 19.8, the total normal stress on the failure plane is:

$$\sigma = \gamma_{sat} h\cos^2\beta \tag{19.16}$$

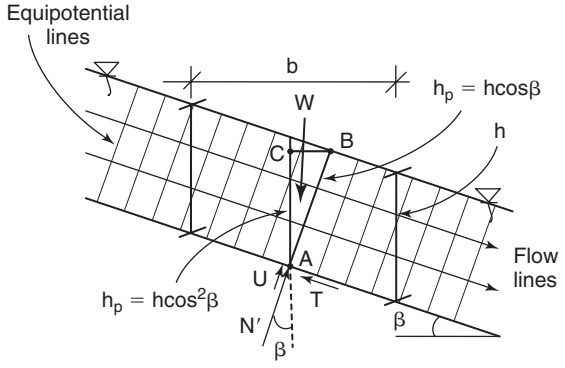

Figure 19.6 Infinite slope with seepage.

where γ_{sat} is the saturated unit weight of the soil. The water stress u_w on the failure is equal to:

$$u_w = h_p \gamma_w \tag{19.17}$$

where h_p is the pressure head on the failure plane.

We know from the flow net properties that the total head at A (Figure 19.6) is equal to the total head at B. We also know that the pressure head at B is zero; therefore, the pressure head at A is the difference in elevation between A and B:

$$h_{tA} = h_{eA} + h_{pA} = h_{tB} = h_{eB} + h_{pB} \tag{19.18}$$

Because h_{pB} is zero, then:

$$h_{pA} = h_{eB} - h_{eA} \tag{19.19}$$

Therefore, the vertical distance AC in Figure 19.6 is the pressure head at A, and from geometry we can calculate:

$$h_{pA} = h\cos^2\beta \quad \text{and} \quad u_w = \gamma_w h\cos^2\beta \tag{19.20}$$

Then the effective stress σ' is:

$$\sigma' = (\gamma_{sat} - \gamma_w)h\cos^2\beta \tag{19.21}$$

and the shear strength is:

$$\tau_f = c' + (\gamma_{sat} - \gamma_w)h\cos^2\beta\tan\varphi' \tag{19.22}$$

so the factor of safety becomes:

$$F = \frac{\tau_f}{\tau} = \frac{c' + (\gamma_{sat} - \gamma_w)h\cos^2\beta\tan\varphi'}{\gamma_{sat}h\sin\beta\cos\beta} = \frac{c'}{\gamma_{sat}h\sin\beta\cos\beta} + \frac{(\gamma_{sat} - \gamma_w)}{\gamma_{sat}}\frac{\tan\varphi'}{\tan\beta} \tag{19.23}$$

19.3.4 $c' - \varphi'$ Soil with Unsaturated Conditions

In the case of $c' - \varphi'$ soil with unsaturated conditions, the effective stress becomes:

$$\sigma' = \gamma_t h\cos^2\beta - \alpha u_w \tag{19.24}$$

The shear strength is now:

$$\tau_f = c' + (\gamma_t h\cos^2\beta - \alpha u_w)\tan\varphi' \tag{19.25}$$

Because the mobilized shear stress remains the same, the factor of safety is:

$$F = \frac{\tau_f}{\tau} = \frac{c' + (\gamma_t h\cos^2\beta - \alpha u_w)\tan\varphi'}{\gamma_t h\sin\beta\cos\beta} = \frac{c'}{\gamma_t h\sin\beta\cos\beta} - \frac{\alpha u_w\tan\varphi'}{\gamma_t h\sin\beta\cos\beta} + \frac{\tan\varphi'}{\tan\beta} \tag{19.26}$$

Comparison

The factors of safety corresponding to the various soil conditions can be compared. Assume that the soil is an overconsolidated silty clay with $c' = 5$ kPa and $\varphi' = 30^\circ$, the slope has an angle of 20° with the horizontal, and the unit weight is 20 kN/m^3. The question is: What is the factor of safety against failure for a plane at a depth 2 m below the ground surface?

For the case of the dry soil, the factor of safety is:

$$F_{dry} = \frac{5}{20\times 2\sin 20\cos 20} + \frac{\tan 30}{\tan 20} = 0.389 + 1.586 = 1.975 \tag{19.27}$$

For the case of the slope with seepage, the factor of safety is:

$$F_{seep} = \frac{5}{20\times 2\sin 20\cos 20} + \frac{(20-10)}{20}\frac{\tan 30}{\tan 20} = 0.389 + 0.793 = 1.182 \tag{19.28}$$

For the case of the slope with an unsaturated condition, with a degree of saturation equal to 60% and a water tension equal to -1000 kPa, the factor of safety is:

$$F_{unsat} = \frac{5}{20\times 2\sin 20\cos 20} - \frac{0.6(-100)\tan 30}{20\times 2\sin 20\cos 20} + \frac{\tan 30}{\tan 20} = 0.389 + 2.695 + 1.586 = 4.67 \tag{19.29}$$

As can be seen, the factors of safety are organized as follows:

$$F_{unsat} > F_{dry} > F_{seep} \tag{19.30}$$

Note that F_{unsat} is much higher than the other factors of safety even though the water tension is quite modest. Therefore, water tension plays a very important role in slope stability. Note also that if there is no cohesion, F_{seep} will be equal to half of F_{dry}. Again the role of water proves to be very important in slope stability. These calculations explain why slope failures are more likely to happen after heavy prolonged rains, as is often reported in the news media.

19.4 SEEPAGE FORCE IN STABILITY ANALYSIS

The *seepage force* is the force exerted in friction by water flowing around soil particles and trying to drag them away. The forces shown on a free-body diagram are the external forces. The internal forces are resolved internally. The seepage force is an external force when the soil skeleton is considered the free body, but it is an internal force when the soil skeleton plus the water are considered the free body. Most slope stability analyses consider the soil skeleton plus the water as the free body. In those cases the seepage force must not be included in any slope stability calculations.

Figure 19.7 shows the two free-body diagram options. In the case where the free body is the soil particles plus the

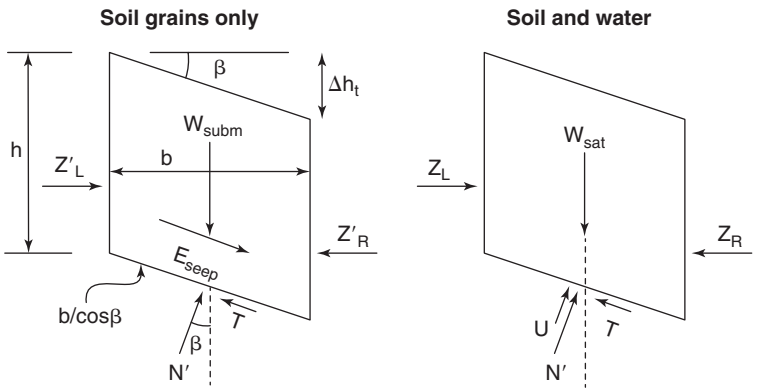

Figure 19.7 Soil skeleton and seepage force approach.

water, the weight W is the total weight including the solids and the water; the side forces are the total forces Z_R and Z_L; and the bottom forces are the effective normal force N′, the uplift force U, and the shear force *T*. In the case where the free body is the soil particles alone, the weight W_{subm} is the total weight minus the buoyancy force, the side forces are the effective components Z'_R and Z'_L, the bottom forces are the effective normal force N′ and the shear force T, and the seepage force E_u must be included.

Let's go back to the example of the infinite slope in the case of seepage through the slope. In the solution presented in the subsection concerning $c' - \varphi'$ soil with seepage, the free body considered was the soil skeleton and the water all together, as is usually done. As you recall, we did not consider the seepage force in that case. Indeed, it was an internal force because it was a force acting between the particles and the water, which are both part of the free body. Let's see what happens if we consider instead the soil skeleton alone to be the free body.

The forces are calculated as follows:

Submerged weight:

$$W_{subm} = (\gamma_{sat} - \gamma_w)bh \tag{19.31}$$

Normal force on bottom:

$$N' = W_{subm}\cos\beta = (\gamma_{sat} - \gamma_w)bh\cos\beta \tag{19.32}$$

Shear force on bottom:

$$T = W_{subm}\sin\beta + E_{seep} \tag{19.33}$$

Normal stress on bottom:

$$\sigma' = \frac{N'}{b/\cos\beta} = (\gamma_{sat} - \gamma_w)h\cos^2\beta \tag{19.34}$$

Uplift force on bottom (Eq. 9.20):

$$U = \gamma_w h\cos^2\beta \times \frac{b}{\cos\beta} \tag{19.35}$$

Seepage force:

$$E_{seep} = i\gamma_w bh \tag{19.36}$$

Hydraulic gradient:

$$i = \frac{\Delta h_t}{b/\cos\beta} = \sin\beta \tag{19.37}$$

Shear stress on bottom:

$$\tau = \frac{T}{b/\cos\beta} = (\gamma_{sat} - \gamma_w)h\sin\beta\cos\beta + \gamma_w h\sin\beta\cos\beta$$
$$= \gamma_{sat}h\sin\beta\cos\beta \tag{19.38}$$

Shear strength on bottom:

$$\tau_f = c' + \sigma'\tan\varphi' = c' + (\gamma_{sat} - \gamma_w)h\cos^2\beta\tan\varphi' \tag{19.39}$$

Then the factor of safety becomes:

$$F = \frac{\tau_f}{\tau} = \frac{c' + (\gamma_{sat} - \gamma_w)h\cos^2\beta\tan\varphi'}{\gamma_{sat}h\sin\beta\cos\beta}$$
$$= \frac{c'}{\gamma_{sat}h\sin\beta\cos\beta} + \frac{(\gamma_{sat} - \gamma_w)}{\gamma_{sat}}\frac{\tan\varphi'}{\tan\beta} \tag{19.40}$$

We get the same result as with Eq. 19.23, but after having started from a different free-body diagram (the free body of the soil skeleton with the water as an outside influence). The simplest approach in slope stability analysis is to consider the soil and the water together. When you do so, the seepage force is an internal force and does not enter into the calculations.

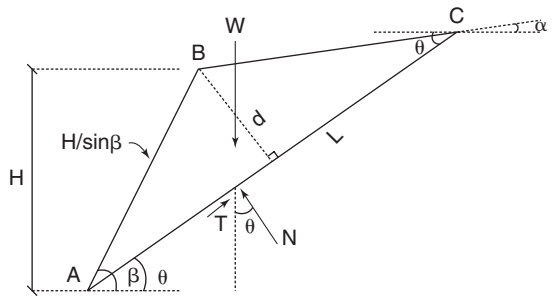

Figure 19.8 Plane failure along the bottom of a wedge.

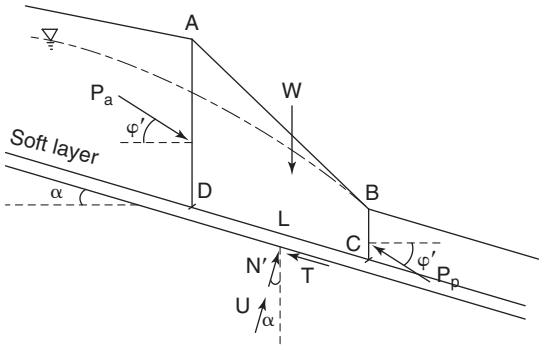

Figure 19.9 Block failure along a plane.

19.5 PLANE SURFACES

The infinite slope is a case of a plane surface. A plane surface can also be considered as the base of a wedge (Figure 19.8). In this case, the factor of safety can be calculated as follows. The length of the side AB of the triangle is H/sin β. Referring to Figure 19.8, the rule of sines in the triangle ABC gives:

$$\frac{H/\sin\beta}{\sin(\theta-\alpha)} = \frac{L}{\sin(\pi-\beta+\alpha)} \tag{19.41}$$

or:

$$L = \frac{H}{\sin\beta}\frac{\sin(\beta-\alpha)}{\sin(\theta-\alpha)} \tag{19.42}$$

Then the height d of the triangle is given by:

$$d = \frac{H}{\sin\beta}\sin(\beta-\theta) \tag{19.43}$$

The weight of the wedge is:

$$W = \frac{1}{2}\gamma Ld = \frac{1}{2}\gamma H^2\frac{\sin(\beta-\theta)\sin(\beta-\alpha)}{\sin^2\beta\sin(\theta-\alpha)} \tag{19.44}$$

The shear force T and normal force N necessary to keep the wedge in equilibrium are:

$$T = W\sin\theta \tag{19.45}$$

$$N = W\cos\theta \tag{19.46}$$

Then the factor of safety is:

$$F = \frac{S}{T} = \frac{c'L + W\cos\theta\tan\varphi'}{W\sin\theta} \tag{19.47}$$

where W is given by Eq. 19.44.

19.6 BLOCK ANALYSIS

Sometimes the most likely failure mechanism is a block of soil moving along a predetermined interface because of the presence of a weak layer along the bottom of the block (Figure 19.9). The stability analysis of block ABCD in Figure 19.9 is called a *block analysis*. In this case the driving shear force T along the potential failure plane DC is:

$$T = W\sin\alpha \tag{19.48}$$

The component of the active force P_a in the direction of sliding along DC is calculated according to the methodology described in Chapter 21. Along AD it is:

$$P_a\cos(\varphi'-\alpha) \tag{19.49}$$

At the same time, the component of the passive resistance P_p in the direction of sliding along BC is calculated according to the methodology described in Chapter 21. Along BC it is:

$$P_p\cos(\varphi'-\alpha) \tag{19.50}$$

The normal force N on the plane of failure is:

$$N = W\cos\alpha \tag{19.51}$$

and the uplift force U due to the average water stress u_w on the potential failure plane is:

$$U = u_wL \tag{19.52}$$

So, the maximum shear resistance on the potential plane of failure is:

$$S = c'L + (W\cos\alpha - u_wL)\tan\varphi' \tag{19.53}$$

The factor of safety against sliding of the block on plane DC can then be calculated as:

$$F = \frac{c'L + (W\cos\alpha - u_wL)\tan\varphi' + P_p\cos(\varphi'-\alpha)}{W\sin\alpha + P_a\cos(\varphi'-\alpha)} \tag{19.54}$$

19.7 SLOPES WITH WATER IN TENSILE CRACKS

Tensile cracks can develop at the top of a slope due either to impending failure or to desiccation. The depth of those cracks is highly variable. The depth of cracks due to desiccation is approximately equal to the horizontal distance between cracks on the ground surface. The depth of cracks due to active

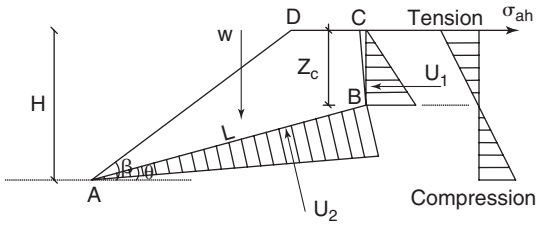

Figure 19.10 Influence of a tension crack at the top of a slope.

pressure failure can be calculated by using the active pressure expression and finding the depth where tension ends and the effective horizontal stress becomes zero (Figure 19.10). The expression for the active effective stress σ'_{ah} is (see Chapter 21):

$$\sigma'_{ah} = \sigma'_{ov} \tan^2\left(45 - \frac{\varphi'}{2}\right) - 2c' \tan\left(45 - \frac{\varphi'}{2}\right) \quad (19.55)$$

Setting Eq. 19.55 equal to zero gives the depth of the tension crack. This requires expressing σ'_{oh} as a function of the depth z. If the water table is at the ground surface, the depth of the crack is:

$$z_c = \frac{2c'}{(\gamma_{sat} - \gamma_w)\tan\left(45 - \frac{\varphi'}{2}\right)} \quad (19.56)$$

If the soil is unsaturated:

$$z_c = \frac{2c'}{\gamma_t \tan\left(45 - \frac{\varphi'}{2}\right)} + \frac{\alpha u_w}{\gamma_t} \quad (19.57)$$

Because u_w is negative, Eq. 19.57 gives a lower estimate of z_c than does Eq. 19.56. As it is rare to have the groundwater table at the ground surface near a slope, z_c is often estimated as:

$$z_c = \frac{2c'}{\gamma_t \tan\left(45 - \frac{\varphi'}{2}\right)} \quad (19.58)$$

Of course, engineering judgment always plays an important role in such decisions. Once an estimate of z_c is known, the slope stability analysis can proceed with the worst-case assumption that the crack is filled with water. Indeed, the water pressure pushes the slope horizontally. Figure 19.10 shows a planar surface analysis. In this case, the water forces U_1 and U_2 are:

$$U_1 = \frac{1}{2}\gamma_w {z_c}^2 \quad (19.59)$$

$$U_2 = \frac{1}{2}\gamma_w z_c L \quad (19.60)$$

The length L of segment AB is given by:

$$L = \frac{H - z_c}{\sin\theta} \quad (19.61)$$

The driving shear force on plane AB is:

$$T = W \sin\theta + U_1 \cos\theta \quad (19.62)$$

The maximum resisting shear force on plane AB is:

$$S = c'L + (W\cos\theta - U_2)\tan\varphi' \quad (19.63)$$

The final expression of the factor of safety is then:

$$F = \frac{c'\dfrac{(H - z_c)}{\sin\theta} + \left(W\cos\theta - \dfrac{1}{2}\gamma_w z_c \dfrac{(H - z_c)}{\sin\theta}\right)\tan\varphi'}{W\sin\alpha + \dfrac{1}{2}\gamma_w z_c^2 \cos\theta} \quad (19.64)$$

19.8 CHART METHODS

When the soil is uniform and a circular failure surface is assumed, the problem is simple enough that the factor of safety can be determined from charts. These charts have been developed by various engineers, including Taylor (1948), Spencer (1967), Janbu (1968), and Morgenstern (1963), among others.

19.8.1 Taylor Chart

Taylor (1948) developed charts for two cases:

- $\varphi' = 0$, undrained shear strength s_u, and total stress analysis
- $\varphi' > 0$, $c' > 0$, no water

$\varphi = 0$, Undrained Shear Strength s_u, and Total Stress Analysis

The slope and its parameters are shown in Figure 19.11. This chart applies where the soil is uniform, can be represented by a constant undrained shear strength s_u, and has a total unit weight γ. Note that the concept $\varphi' = 0$ is not a true concept; however, it is mathematically convenient, and simply expresses the fact that the undrained shear strength is assumed to be independent of the normal total stress. In fact,

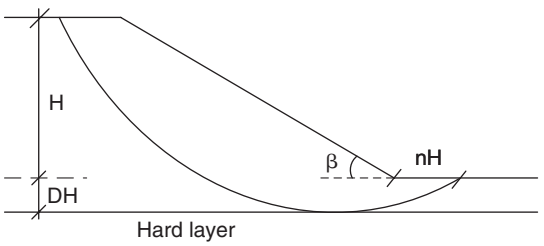

Figure 19.11 Slope parameters for Taylor chart.

φ' is always nonzero, as friction always exists between two materials. However, because the total stress changes and the effective stress does not, it looks like the friction angle is zero; this is why it is more appropriate to say that the total stress friction angle φ is zero whereas φ' is not.

The procedure is as follows:

1. Find the depth factor D, the height of the slope H, the total unit weight γ of the soil, the undrained shear strength s_u of the soil, and the slope angle β. The depth factor D (Figure 19.11) is the ratio between the vertical distance from the toe of the slope to the underlying hard layer and the height of the slope.

2. Knowing D and β, find the stability number N on the chart in Figure 19.12 by using the solid lines. The short dashed lines across the solid lines give the value of n, which is the ratio between the horizontal distance from the toe of the slope to the exit of the circle and the height of the slope. Once n is known, the circle can be identified, because it must be tangent to the hard layer.

3. The stability number N is defined as:

$$N = \frac{c_d}{\gamma H} \tag{19.65}$$

where c_d is the shear stress necessary to keep the slope in equilibrium. Using Eq. 19.65, calculate the value of c_d.

4. The factor of safety is given by:

$$F = \frac{s_u}{c_d} \tag{19.66}$$

5. If the geometry of the case at hand is such that the failure circle is most likely to be a toe circle, use the long dashed lines to find the stability number N.

$\varphi' > 0, c' > 0$, No Water, Effective Stress Analysis

This chart (Figure 19.13) applies to the case in which the soil is uniform, has a unit weight γ, has no water, and can be represented by an effective stress cohesion c' and an effective stress friction angle φ'. Note that the statement was that the soil has no water rather than that the soil was dry. Indeed, a dry soil can have enough water to develop very high water tension, which changes the shear strength significantly; this chart refers to the case of no water. For this chart, two factors of safety are defined:

$$F_{c'} = \frac{c'}{c'_d} \quad \text{and} \quad F_{\varphi'} = \frac{\tan\varphi'}{\tan\varphi'_d} \tag{19.67}$$

where c'_d and φ'_d are the fraction of c' and φ' required to maintain the slope in equilibrium.

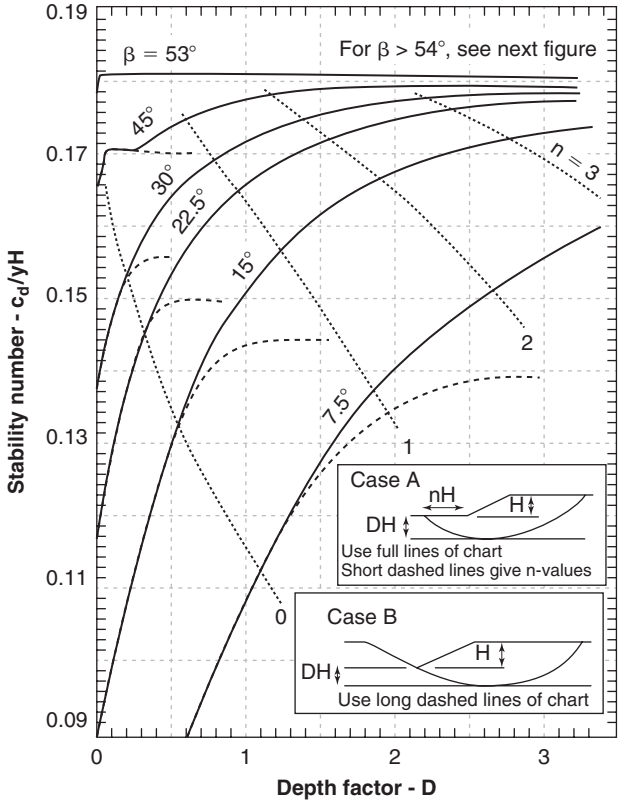

Figure 19.12 Taylor chart for $\varphi = 0$, undrained shear strength s_u soils (Taylor 1948). (This material is reproduced with permission of John Wiley & Sons, Inc.)

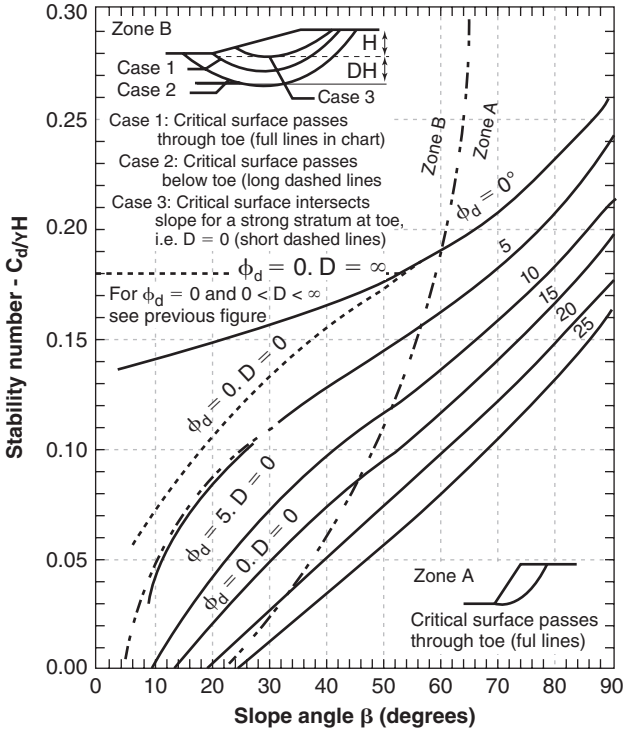

Figure 19.13 Taylor chart for $\varphi' > 0, c' > 0$. no water soils (Taylor 1948). (This material is reproduced with permission of John Wiley & Sons, Inc.)

The step-by-step procedure is as follows:

1. Choose an initial value of F'_c. A value of 1.5 is common.
2. Using Eq. 19.67, calculate the value of c'_d.
3. Calculate the depth factor D as defined in Figure 19.11 and the stability factor N as:

$$N = \frac{c'_d}{\gamma H} \tag{19.68}$$

4. Knowing the stability number N, the slope angle β, and the depth factor D, find φ'_d from the chart. Use the solid lines for the general case and the other lines as appropriate; check the chart for details.
5. Calculate F'_φ and compare to F'_c.
6. If F'_φ and F'_c are not equal or within a target tolerance, go back to step 1 and try a new value of F'_c until they are within that tolerance. It would be reasonable to use the mean of F'_c and F'_φ as the next guess.

19.8.2 Spencer Chart

Spencer (1967) developed charts for the case where the groundwater surface is within the slope circle (Figure 19.14). The soil strength is described by the effective stress parameters c' and φ'. The failure surface is considered to be circular and to go through the toe of the slope. The presence of the water in the slope is quantified by using the water stress ratio r_u:

$$r_u = \frac{u_w}{\sigma_{ov}} \tag{19.69}$$

where u_w is the water stress at the chosen point and σ_{ov} is the vertical total stress in the soil at the same point. Although r_u varies from one point to the next in the slope, a single value is used for the chart method. Referring to Figure 19.14 the average ratio r_u is estimated as:

$$r_u = \frac{\gamma_w}{\gamma_t} \times \frac{Area\ \ ABGEF}{Area\ \ ABCDEF} \tag{19.70}$$

where γ_w and γ_t are the unit weight of water and the total unit weight of the soil respectively. Note that the maximum value of r_u is about 0.5, because even if the slope is filled with water the ratio γ_w/γ_t is about 0.5. As a result, Spencer prepared charts for values of $r_u = 0$ (slope with no water), $r_u = 0.25$ (slope with water halfway up), and $r_u = 0.5$ (slope full of water). Note also that there is no water outside the slope.

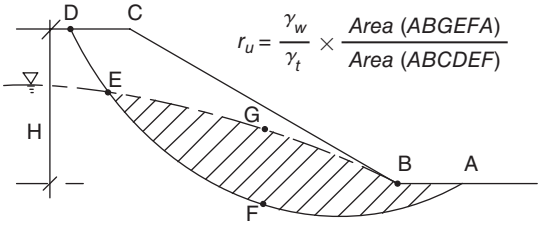

Figure 19.14 Slope parameters for Spencer chart.

The procedure for using Spencer's chart is as follows:

1. Choose an initial value of F'_c (Eq. 19.67). A value of 1.5 is common.
2. Using Eq. 19.67, calculate the value of c'_d.
3. Calculate the stability factor N as:

$$N = \frac{c'_d}{\gamma H} \tag{19.71}$$

4. Calculate the water stress ratio r_u.
5. Knowing the stability number N, the water stress ratio r_u, and the slope angle β, find φ'_d from the chart (Figure 19.15). If the ratio r_u is not exactly equal to 0, 0.25, or 0.5 as in the charts, the two closest cases of ratio r_u are calculated and interpolation on F'_φ is used.
6. Calculate F'_φ and compare to F'_c.
7. If F'_φ and F'_c are not equal or within a target tolerance, go back to step 1 and try a new value of F'_c until F'_φ and F'_c are within that tolerance. Using the mean of F'_c and F'_φ as the next guess for F'_c is reasonable.

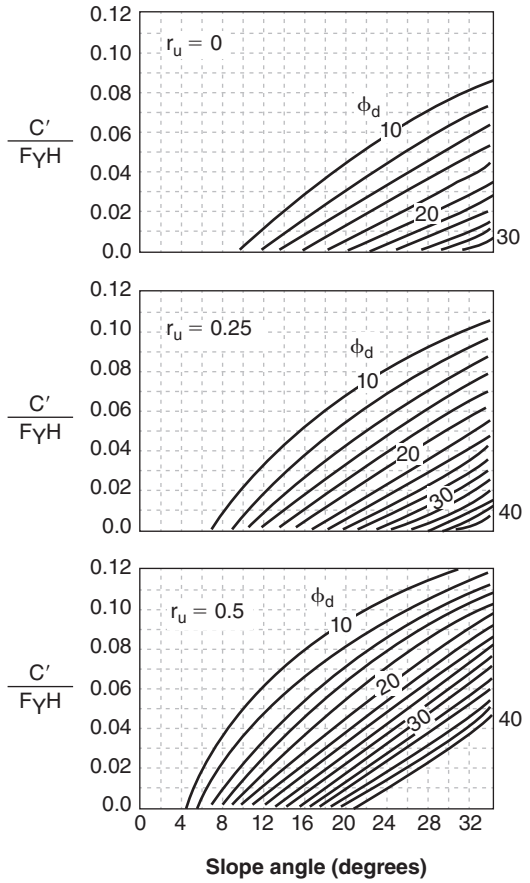

Figure 19.15 Spencer chart for $\varphi' > 0$, $c' > 0$. water in slope soils (Spencer 1967). (This material is reproduced with permission of John Wiley & Sons, Inc.)

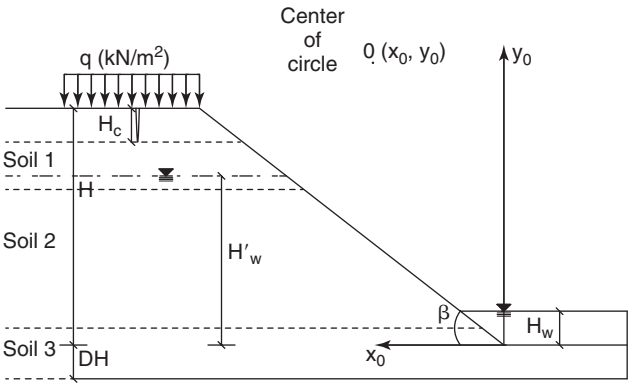

Figure 19.16 Slope parameters for Janbu chart.

19.8.3 Janbu Chart

Janbu (1968) developed an extensive set of charts covering many different cases. They include charts for the case where the soil has several layers, charts for the case where a surcharge exists on top of the slope, charts where a crack exists at the top of the slope, charts dealing with undrained short-term behavior, charts dealing with effective stress drained behavior, and charts dealing with different water levels outside the slope and inside the slope (Figure 19.16). These charts are detailed in Abramson et al. (2002) and in Duncan and Wright (2005). The chart dealing with a uniform soil, effective stress parameters c′ and φ', different water levels inside and outside the slope, and toe circles as failure surfaces is discussed here.

The procedure is as follows:

1. Calculate P_d as:

$$P_d = \frac{\gamma H + q - \gamma_w H_w}{\mu_q \mu_w \mu_t} \tag{19.72}$$

where P_d is a stress parameter characterizing the demand side of the slope stability; γ is the total unit weight of the soil; H is the height of the slope; q is the uniform surcharge at the top of the slope; γ_w is the unit weight of water; H_w is the height of water outside of the slope above the toe of the slope (Figure 19.16); and μ_q, μ_w, and μ_t are reduction factors for the surcharge, the submergence, and the tension crack respectively. In the case of no surcharge, μ_q is 1; in the case of no tension cracks, μ_t is 1 as well. The value of μ_w is found in the chart shown in Figure 19.17.

2. Calculate the effective stress parameter P_e as:

$$P_e = \frac{\gamma H + q - \gamma_w H'_w}{\mu_q \mu'_w} \tag{19.73}$$

where P_e is an effective stress parameter characterizing the average effective stress on the failure plane, γ is the total unit weight of the soil, H is the height of the slope, q is the uniform surcharge at the top of the slope, γ_w is the unit weight of water, H'_w is the height of water within the slope above the toe of the slope (Figure 19.16), and μ_q and μ'_w are the surcharge reduction factor and the seepage factor respectively. In the case of no surcharge, μ_q is 1 and the value of μ'_w is found in the chart shown in Figure 19.17.

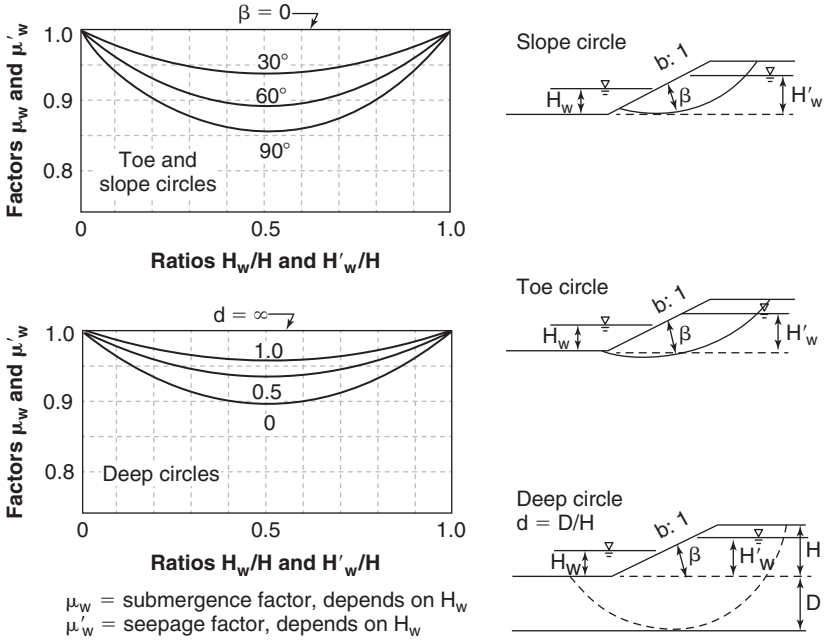

Figure 19.17 Janbu chart for the submergence reduction factor μ_w and μ'_w (Janbu 1968). (This material is reproduced with permission of John Wiley & Sons, Inc.)

3. Calculate $\lambda_{c\varphi}$ as:

$$\lambda_{c\varphi} = \frac{P_e \tan \varphi'}{c'} \tag{19.74}$$

where $\lambda_{c\varphi}$ is a parameter characterizing the ratio between the strength due to friction over the strength due to cohesion, and c' and φ' are the effective stress cohesion and friction angle respectively.

4. Using the chart in Figure 19.18, together with the slope angle β and the strength ratio $\lambda_{c\varphi}$, determine the stability number N_{cf}.

5. Calculate the factor of safety as:

$$F = N_{cf} \frac{c'}{P_d} \tag{19.75}$$

6. The location of the center of the failure circle is given by the chart in Figure 19.19. The chart gives the normalized values x_o and y_o of the coordinates:

$$X_o = x_o H \quad and \quad Y_o = y_o H \tag{19.76}$$

where X_o and Y_o are the actual coordinates in meters, and H is the height of the slope.

19.8.4 Morgenstern Chart

Morgenstern (1963) developed charts for the case of a rapid drawdown in a dam (Figures 19.20 and 19.21). The charts are for a uniform soil slope, effective stress parameters c′ and φ', soil total unit weight γ, a slope with a height H, and the

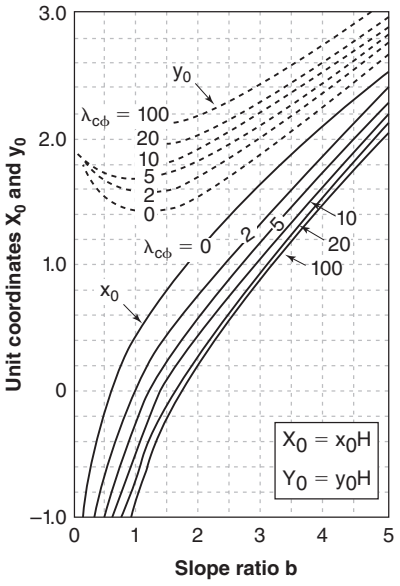

Figure 19.19 Janbu chart for locating the center of the critical circle. (After Janbu 1968. From J. Michael Duncan and Stephen G. Wright, *Soil Strength and Slope Stability*, Hoboken, NJ, John Wiley & Sons, 2005. This material is reproduced with permission of John Wiley & Sons, Inc.)

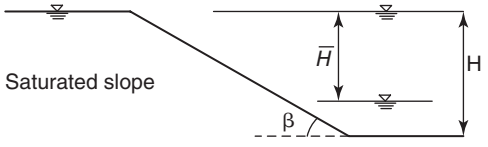

Figure 19.20 Slope parameters for Morgenstern chart: *(a)* $c'/\gamma H = 0.0125$. *(b)* $c'/\gamma H = 0.025$.

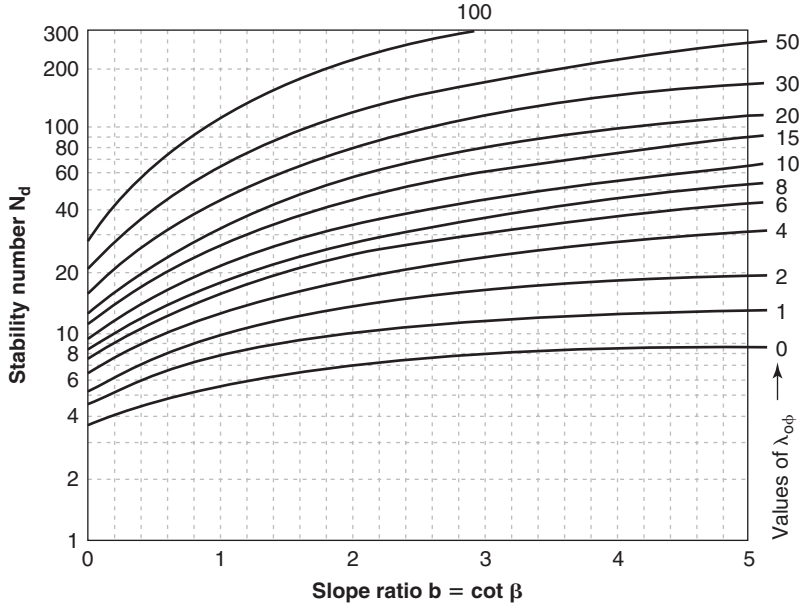

Figure 19.18 Janbu chart for obtaining the stability factor. (After Janbu 1968. From J. Michael Duncan and Stephen G. Wright, *Soil Strength and Slope Stability*, Hoboken, NJ, John Wiley & Sons, 2005. This material is reproduced with permission of John Wiley & Sons, Inc.)

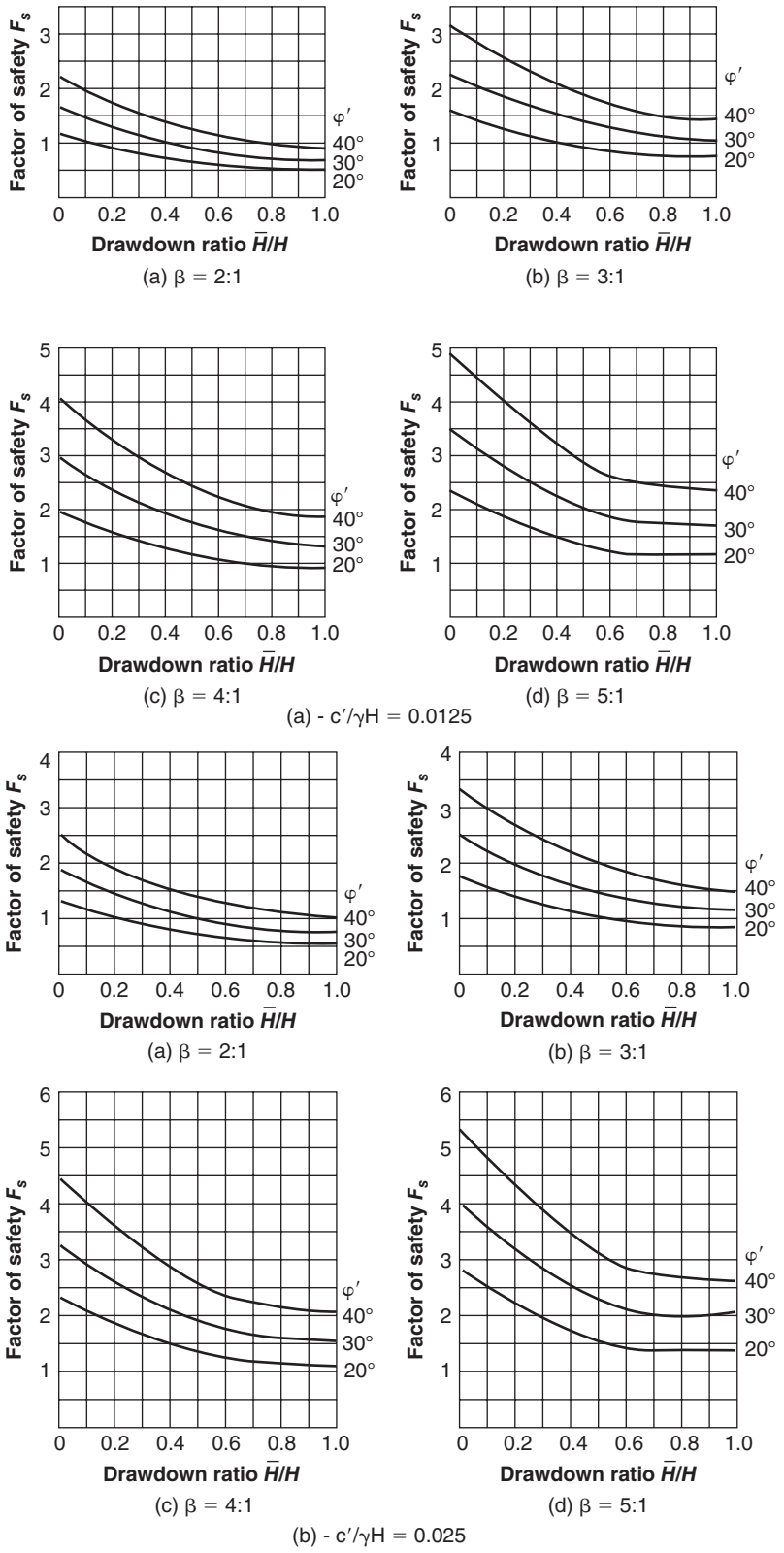

Figure 19.21 Morgenstern chart for rapid drawdown. (After Morgenstern 1963. *a* and *b*: From L. W. Abramson et al., *Slope Stability and Stabilization Methods* (1st ed.), Hoboken, NJ, John Wiley & Sons, 1996. This material is reproduced with permission of John Wiley & Sons, Inc.)

water level being drawn down an amount $\overline{H}$ from the top of the slope to a lower level. It is further assumed that the water stress in the soil does not have time to dissipate during the drawdown period.

The procedure is as follows:

1. Calculate the quantities $c'/\gamma H$ and $\tan \beta$.
2. Select the chart that corresponds to the correct $c'/\gamma H$, and the correct $\tan \beta$.
3. Using the values of $\overline{H}/H$ and φ', find the value of the factor of safety on the chart.

19.9 METHOD OF SLICES

The method of slices avoids some of the limitations associated with the chart methods. The method of slices is applicable to layered soils and to any water stress distribution. It is still associated with circular failure surfaces, although the concept can be applied to other shapes. The origin of the method goes back to the work of Fellenius (1927), a Swedish engineer. This problem-solving approach proceeds by breaking down the mass of soil into elements, drawing a free-body diagram of each element, writing the constitutive and fundamental equations at the element level, solving for the unknowns, and reassembling the pieces once the forces are known at the element level. Recall that what we really want to evaluate is the factor of safety of the slope F as defined in Eq. 19.1. In the method of slices, the soil mass is sliced as shown in Figure 19.22. Typically a minimum of 10 slices is necessary for reasonable accuracy. Figure 19.23 shows a slice with all parameters indicated. These parameters are defined in Table 19.1.

The number of unknowns and the number of equations available to find the values of the unknowns must be evaluated. The soil properties and the geometry of the slope are known quantities. The known forces are Q, U_β, W, k_h, k_v, and U_θ, whereas the known distances are b, h, and h_C. Furthermore, it is commonly assumed that the reactions N' and U_θ are acting at the midpoint of the bottom of the slice while

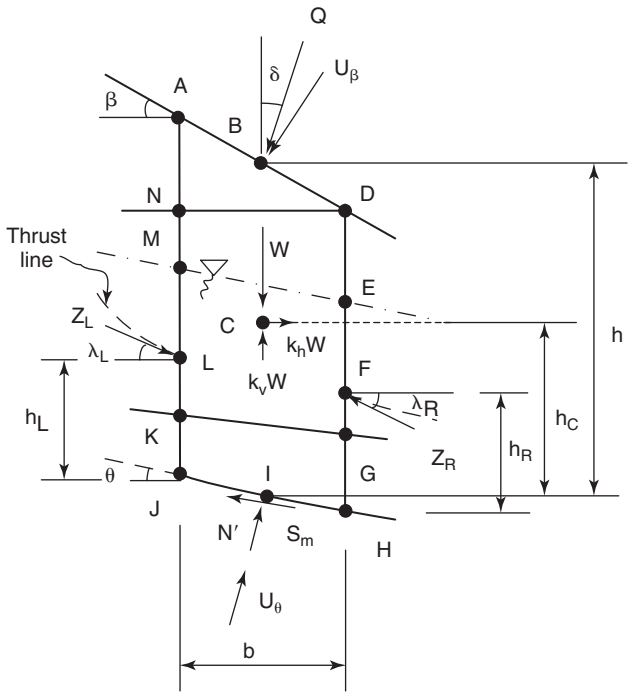

Figure 19.23 Slope slice i.

Q and U_β are applied at the middle of the top of the slice. The number of unknowns and the number of equations are shown in Table 19.2.

The total number of unknowns is 5n−2 and the total number of equations is 4n; therefore, there are n−2 unknowns in excess and the problem is statically indeterminate. It is necessary to make assumptions. Many assumptions have been made over time and each set of assumptions has been associated with one of the methods of slices. The assumptions and the associated names are presented in Table 19.3. That table shows the progress that took place over a period of 50 years in reducing the coarseness of the assumptions and increasingly satisfying the fundamental equations. The ordinary method of slices, the Bishop simplified method, and the generalized

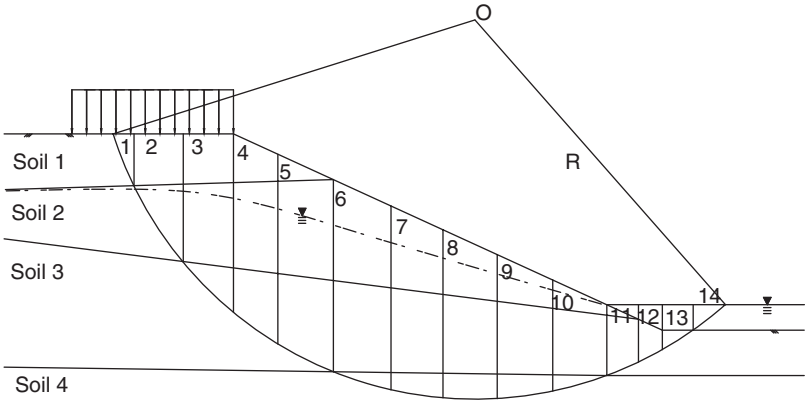

Figure 19.22 Sliced slope.

Table 19.1 Definition of Parameters in Figure 19.23

Q = force applied at the top of the slice	δ = angle of force Q with the vertical
U_β = water force applied at top of slice	θ = angle of bottom of slice with horizontal
W = total weight of slice	β = angle of top of slice with horizontal
$k_h W$ = horizontal static force due to earthquake	λ_L = angle of force Z_L with horizontal
$k_v W$ = vertical static force due to earthquake	λ_R = angle of force Z_R with horizontal
Z_L = earth pressure force on left side of slice	h_L = height of point of application of Z_L above bottom of left side of slice
Z_R = earth pressure force on right side of slice	h_R = height of point of application of Z_R above bottom of right side of slice
S_m = mobilized shear force at bottom of slice	h_C = height of center of gravity of slice above the middle of the bottom of slice
N′ = normal force on base of slice transmitted through the grains	h = height of slice from center of bottom to center of top
U_θ = water force applied at bottom of slice	b = width of slice

limit equilibrium method are detailed next. The other methods are presented in Abramson et al. (2002) and in Duncan and Wright (2005).

19.9.1 Ordinary Method of Slices

The assumption made by Fellenius (1927) is that the resultant of Z_L and Z_R (Figure 19.23) is equal to zero. This assumption decreases the number of unknowns by $3n - 3$ (Table 19.2), leaving $2n + 1$ unknowns and 4n equations. Therefore, the system is overdeterminate, meaning that not all equations can be satisfied. Fellenius chose to satisfy equilibrium of each slice in a direction perpendicular to the bottom of the slice. Referring to Figure 19.23, this leads to the following expression for slice i:

$$N_i' + U_{\theta i} + k_h W_i \sin\theta_i - W_i(1 - k_v)\cos\theta_i - U_{\beta i}\cos(\beta_i - \theta_i) - Q_i \cos(\delta_i - \theta_i) = 0 \qquad (19.77)$$

Table 19.2 Unknowns and Equations for the Method of Slices

Unknowns	Equations
n values of S_m forces	n force equilibrium equations in x direction
n values of N′	n force equilibrium equations in y direction
n − 1 values of Z forces	n moment equilibrium equations
n − 1 values of the angles λ	n shear strength equation
n − 1 values of the location of the Z forces	
1 factor of safety	
TOTAL = $5n - 2$	TOTAL = $4n$

This equation gives the expression of N_i'.

The value of $U_{\theta i}$ is given by:

$$U_{\theta i} = \alpha_i u_{wi} \frac{b_i}{\cos\theta_i} \qquad (19.78)$$

where α_i is the area ratio for the soil along the bottom of the slice (see section 15.5) and u_{wi} is the average water stress at the bottom of the slice. Obtaining the value u_{wi} is discussed in section 19.10. The weight of the slice W_i is calculated using the total unit weight of the soil. If the slice includes several soil layers, the weight is given by:

$$W_i = \sum_{j=1}^{m} \gamma_j A_j \qquad (19.79)$$

where γ_j is the total unit weight of soil j within slice i and A_j is the area of soil j included within slice i.

The expression for the mobilized shear force at the bottom of slice i necessary to keep the slope in equilibrium S_{mi} is given by the shear strength equation and the factor of safety:

$$S_{mi} = \frac{c_i' \frac{b_i}{\cos\theta_i} + N_i' \tan\varphi_i'}{F} \qquad (19.80)$$

where F is the global factor of safety for the slope. Then the global factor of safety F for the n slices in the slope is given by the ratio between the global maximum resisting moment $M_{R\max}$ around O, the center of the circle, and the global driving moment M_D around O:

$$F = \frac{M_{R\max}}{M_D} \qquad (19.81)$$

The expressions for $M_{R\max}$ and M_D are:

$$M_{R\max} = \sum_{i=1}^{n} \left(c_i' \frac{b_i}{\cos\theta_i} + N_i' \tan\varphi_i' \right) R \qquad (19.82)$$

Table 19.3 Methods of Slices, Authors, and Assumptions

Name of Method	Reference	Assumptions	Comment
Ordinary method of slices	Fellenius 1927	Resultant of Z forces on each slice is equal to zero.	Based on writing equilibrium perpendicular to base. Does not satisfy all equilibrium equations. Overdeterminate.
Janbu simplified method	Janbu 1954	Z forces are horizontal.	Does not satisfy all equilibrium equations. Overdeterminate.
Bishop simplified method	Bishop 1955	Shear forces on the side of all slices are zero (i.e., Z forces are horizontal).	Based on writing vertical force equilibrium. Does not satisfy all equilibrium equations. Overdeterminate.
Bishop rigorous method	Bishop 1955	Shear forces on the side of all slices are assumed.	Satisfies all equilibrium equations.
Lowe and Karafiath method	Lowe and Karafiath 1960	Z_R forces inclined at an angle equal to the average between the angle of the top and bottom of the slice.	Does not satisfy all equilibrium equations.
Morgenstern-Price method	Morgenstern and Price 1965	Inclination of Z forces given by a function of the horizontal distance multiplied by a scalar.	Satisfies all equilibrium equations.
Spencer method	Spencer 1967	Z forces have a constant but unknown inclination.	Satisfies all equilibrium equations.
Corps of Engineers method	U.S. Army Corps of Engineers 1970	Z forces inclined parallel to the ground surface or parallel to the line joining the beginning and the end of the failure circle.	Does not satisfy all equilibrium equations.
Janbu generalized method	Janbu 1973	Location of point of application of the Z forces on an assumed thrust line.	Does not satisfy all equilibrium equations.
Sarma method	Sarma 1973	Inclination of Z forces given by a function of the horizontal distance multiplied by a scalar.	Makes use of horizontal seismic coefficient. Satisfies all equilibrium equations.

$$M_D = \sum_{i=1}^{n} \left[\begin{array}{l} \left(W_i \left(1 - k_v\right) + U_{\beta i} \cos \beta_i + Q_i \cos \delta_i\right) \\ \quad \times R \sin \theta_i - \left(U_{\beta i} \sin \beta_i + Q_i \sin \delta_i\right) \\ \quad \times \left(R \cos \theta_i - h_i\right) + k_h W_i \left(R \cos \theta_i - h_{ci}\right) \end{array} \right] \tag{19.83}$$

and the general expression of the factor of safety for the ordinary method of slices is:

$$F = \frac{\displaystyle\sum_{i=1}^{n} \left(\begin{array}{l} c_i' \dfrac{b_i}{\cos \theta_i} + \left(W_i \left(1 - k_v\right) \cos \theta_i \right. \\ \quad + U_{\beta i} \cos(\beta_i - \theta_i) + Q_i \cos(\delta_i - \theta_i) - U_{\theta i} \\ \quad \left. - k_h W_i \sin \theta_i\right) \tan \varphi_i' \end{array} \right) R}{\displaystyle\sum_{i=1}^{n} \left[\begin{array}{l} \left(W_i \left(1 - k_v\right) + U_{\beta i} \cos \beta_i + Q_i \cos \delta_i\right) \\ \quad \times R \sin \theta_i - \left(U_{\beta i} \sin \beta_i + Q_i \sin \delta_i\right) \\ \quad \times \left(R \cos \theta_i - h_i\right) + k_h W_i \left(R \cos \theta_i - h_{ci}\right) \end{array} \right]} \tag{19.84}$$

In the simple case where $k_h = k_v = U_{\beta \mathrm{i}} = Q_i = 0$ (no earthquake, no water on top of ground surface, no structures on top of ground surface), the expression of the factor of safety becomes:

$$F = \frac{\displaystyle\sum_{i=1}^{n} \left(c_i' \frac{b_i}{\cos \theta_i} + \left(W_i \cos \theta_i - \alpha_i u_{wi} \frac{b_i}{\cos \theta_i} \right) \tan \varphi_i' \right)}{\displaystyle\sum_{i=1}^{n} W_i \sin \theta_i} \tag{19.85}$$

The sequential steps to be followed to obtain F correspond to the columns in Table 19.4.

Then the factor of safety is given by:

$$F = \frac{\textit{Sum of column } 14}{\textit{Sum of column } 6} \tag{19.86}$$

Table 19.4 Hand Calculations for the Ordinary Method of Slices (Simple Case of No Earthquake, No Water above Ground Surface, and No Structural Load on Ground Surface)

1	2	3	4	5	6	7	8	9	10	11	12	13	14
Slice no.	Area	Unit weight	W	θ	W sin θ	W cos θ	b/ cos θ	α	u_w	tan ϕ'	c′	$7-8\times 9\times 10$	$8\times 12+13\times 11$
	m^2/m	kN/m^3	kN/m	°	kN/m	kN/m	m		kN/m^2		kN/m^2	kN/m	kN/m
1													
—													
i	$A_1, \ldots,$ $A_j, \ldots,$ A_m	$\gamma_1, \ldots,$ $\gamma_j, \ldots,$ γ_m											
—													
n													

The following notes are very important:

1. Make a drawing to scale of the slope, including the groundwater level and the external loads. This is necessary because the areas in column 2 are measured on the drawing.
2. Choose the circle to be analyzed.
3. Use a minimum of 10 slices and make the slices correspond to natural intersections with the chosen failure circle.
4. The unit weights in column 3 are total unit weights. This means that the seepage force is considered an internal force and must not be included in the calculations.
5. One way to handle a free water body (river, lake) on top of the ground surface is to let the circle cut through the water body, which then becomes part of the free-body diagram. Then, if there is water on top of a slice, the weight of that volume of water must be included in the total weight W in column 4. If water at the end of the circle is considered (e.g., Figure 19.22), then the last slice is a water slice with weight but zero values for c′ and φ'.
6. An alternative way to consider a free water body on top of the ground surface is to consider that the free body stops at the ground surface and to treat the water on top of this body as an external load with weight and direction. This is the way it is presented in Figure 19.23. External loads (due, for example, to structures on the slope surface) are handled in this fashion.
7. The angle θ in column 5 must carry a sign, which will affect the sign of the columns with θ in them. Column 6 will often be affected by the sign of θ; the negative sign of θ indicates that the slice decreases the driving moment of the soil mass.
8. Tan φ' and c′ must be the soil properties at the bottom of the slice, not the average properties of the soil within the slice. The reason is that the shear strength is being evaluated at the bottom of the slice.
9. The quantity in Column 13 for a given slice cannot be negative. If it is and if the calculations are correct, set it equal to zero.

19.9.2 Bishop Simplified Method

The assumption made by Bishop (1955) is that the Z forces (Z_L and Z_R in Figure 19.23) are horizontal. This assumption decreases the number of unknowns by $n-1$, because the angles λ are known (Table 19.2), leaving $4n-1$ unknowns and $4n$ equations. Therefore, the system is overdeterminate by one, meaning that not all equations can be satisfied. Bishop chose to satisfy equilibrium of each slice in the vertical direction. Referring to Figure 19.23, this leads to the following expression for slice *i*:

$$(N_i' + U_{\theta i})\cos\theta_i + S_{mi}\sin\theta_i - W_i(1-k_v) - U_{\beta i}\cos\beta_i - Q_i\cos\delta_i = 0 \tag{19.87}$$

The expression of S_{mi} remains the same as in the OMS (Eq. 19.80). By combining Eq. 19.87 with the expression of S_{mi} (Eq. 19.80), the following expression of N_i'. is obtained:

$$N_i' = \frac{1}{m_{\theta i}}\left(W_i\left(1-k_v\right) - \frac{c_i'\dfrac{b_i}{\cos\theta_i}\sin\theta_i}{F} - U_{\theta i}\cos\theta_i + U_{\beta i}\cos\beta_i + Q_i\cos\delta_i\right) \tag{19.88}$$

with (Figure 19.24):

$$m_{\theta i} = \cos\theta_i\left(1 + \frac{\tan\theta_i\tan\varphi'}{F}\right) \tag{19.89}$$

The expressions of $U_{\theta i}$, W_i, F, M_{Rmax}, and M_D are given by the same equations as in the OMS (Eqs. 19.78, 19.79,

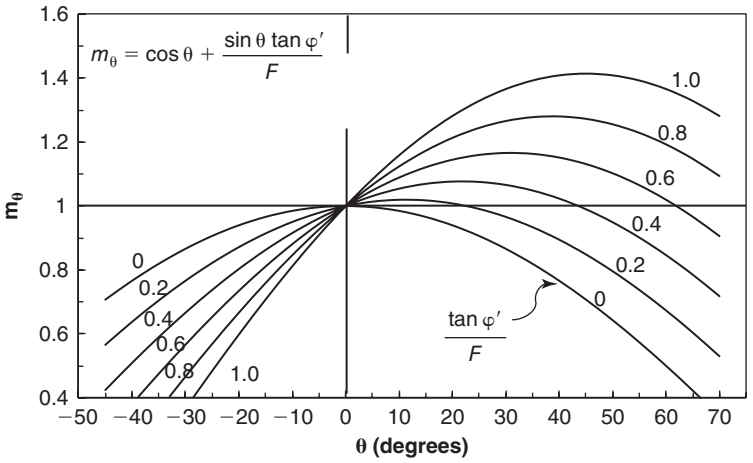

Figure 19.24 Graphical values of the parameters m_θ.

19.81, 19.82, and 19.83 respectively). The only thing that changes is the expression of N′. The final expression of the factor of safety is:

$$F = \frac{\sum_{i=1}^{n} \left(c_i' \frac{b_i}{\cos\theta_i} + \left(\frac{1}{m_{\theta i}} \left(W_i \left(1 - k_v\right) - \frac{c_i' b_i \tan\theta_i}{F} \right) \right) \right) R}{\sum_{i=1}^{n} \left[\begin{array}{c} \left(W_i \left(1 - k_v\right) + U_{\beta i} \cos\beta_i + Q_i \cos\delta_i\right) \\ R \sin\theta_i - \left(U_{\beta i} \sin\beta_i + Q_i \sin\delta_i\right) \\ \times \left(R\cos\theta_i - h_i\right) + k_h W_i \left(R\cos\theta_i - h_{ci}\right) \end{array} \right]} \quad (19.90)$$

In the simple case where $k_h = k_v = U_{\beta i} = Q_i = 0$ (no earthquake, no water on top of ground surface, no structures on top of ground surface), the expression of the factor of safety becomes:

$$F = \frac{\sum_{i=1}^{n} \frac{1}{m_{\theta i}} \left(c_i' b_i + \left(W_i - \alpha_i u_{wi} b_i \right) \tan\varphi_i' \right)}{\sum_{i=1}^{n} W_i \sin\theta_i} \quad (19.91)$$

The sequential steps to be followed to obtain F correspond to the columns in Table 19.5.

Iterations are continued until two consecutive factors of safety fall within the target tolerance.

19.9.3 Generalized Equilibrium Method

Many other methods exist that make various assumptions about the side forces Z_L and Z_R, their inclination, and their location. The generalized equilibrium method (Abramson et al. 2002) exemplifies the general approach. In this method, the inclination angle λ of the side forces is assumed to be described by a function expressed as:

$$\lambda_i = \eta f(x_i) \quad (19.92)$$

where η is a scalar constant for the slope and $f(x_i)$ is the function with values between 0 and 1 describing the variation of the side forces angle λ_i as a function of the horizontal distance x_i along the slope. Examples of the function f(x) are shown in Figure 19.25.

Equation 19.92 decreases the number of unknowns by $n - 1$, as it gives the value of the interslice forces inclinations λ_i, but it does introduce one more unknown in η for a total reduction of unknowns of $n - 2$. This brings down the total number of unknowns to exactly 4n, which now corresponds exactly to the 4n number of equations available. Hence, the system is statically determinate. The equations are similar to those of the Bishop simplified method except that the side forces are now included. Force equilibrium parallel to the base gives n equations:

$$\begin{aligned} &S_{mi} + Z_{Li}\cos(\theta_i - \lambda_{Li}) - Z_{Ri}\cos(\theta_i - \lambda_{Ri}) \\ &\quad - W_i(1 - k_v)\sin\theta_i - W_i k_h \cos\theta_i - U_{\beta i}\sin(\theta_i - \beta_i) \\ &\quad - Q_i \sin(\theta_i - \delta_i) = 0 \end{aligned} \quad (19.93)$$

Force equilibrium perpendicular to the base gives n equations:

$$\begin{aligned} &N_i' + Z_{Ri}\sin(\theta_i - \lambda_{Ri}) - Z_{Li}\sin(\theta_i - \lambda_{Li}) \\ &\quad - W_i(1 - k_v)\cos\theta_i + W_i k_h \sin\theta_i + U_{\theta i} \\ &\quad - U_{\beta i}\cos(\theta_i - \beta_i) - Q_i \cos(\theta_i - \delta_i) = 0 \end{aligned} \quad (19.94)$$

Moment equilibrium around the point at the middle of the base leads to n equations:

$$\begin{aligned} &Z_{Li}\cos\lambda_{Li}\left(h_{Li} - \frac{b_i}{2}\tan\theta_i\right) - Z_{Ri}\cos\lambda_{Ri}\left(h_{Ri} + \frac{b_i}{2}\tan\theta_i\right) \\ &\quad + Z_{Li}\frac{b_i}{2}\sin\lambda_{Li} + Z_{Ri}\frac{b_i}{2}\sin\lambda_{Ri} - W_i k_h h_{ci} + U_{\beta i} h_i \sin\beta_i \\ &\quad + Q_i h_i \sin\delta_i = 0 \end{aligned} \quad (19.95)$$

Table 19.5 Hand Calculations for Bishop Simplified Method (Simple Case of No Earthquake, No Water above Ground Surface, and No Structural Load on Ground Surface)

1	2	3	4	5	6	7	8	9	10	11	12
Slice no.	Area	Unit weight	W	θ	W sin θ	b	α	u_w	tan φ'	c'	$11 \times 7 + (4 - 8 \times 9 \times 7) \times 10$
	m^2/m	kN/m^3	kN/m	°	kN/m	m		kN/m^2		kN/m^2	kN/m
1											
...											
i	$A_1, \ldots,$ $A_j, \ldots,$ A_m	$\gamma_1, \ldots,$ $\gamma_j, \ldots,$ γ_m									
...											
n											

13	14	15	16	17	18	19
Choose $F_1 = 1.5$?	$m_{\theta 1}$ = Eq. 19.85 or Figure 19.24	12/14	$F_2 = \Sigma 15 / \Sigma 6$	$m_{\theta 2}$ = Eq. 19.85 or Figure 19.22 using F_2	12/17	$F_3 = \Sigma 18 / \Sigma 6$

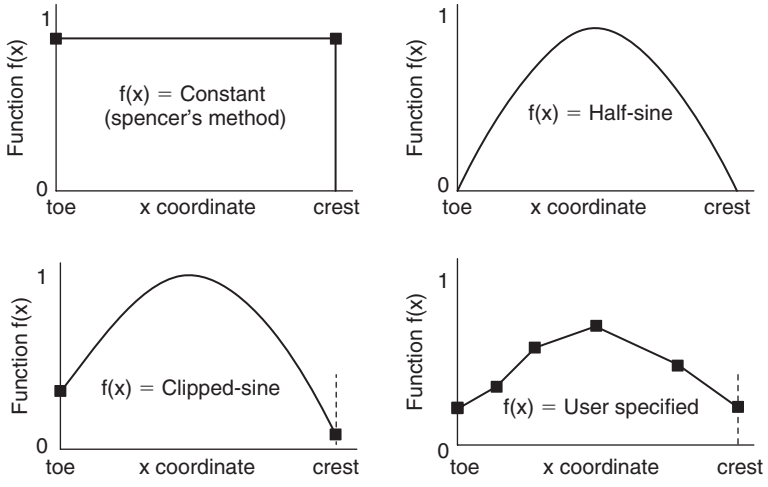

Figure 19.25 Example of functions f(x) (after Abramson et al., 2002).

Then one can write n shear strength equations:

$$S_{mi} = \frac{c'_i \dfrac{b_i}{\cos\theta_i} + N'_i \tan\varphi'_i}{F} \tag{19.96}$$

These 4n equations contain $4n$ unknowns, which are the n values of the S_m forces, the n values of the N' forces, the $n-1$ values of the Z forces, the $n-1$ values of the location of the Z forces, the scalar η, and the factor of safety F. The system is solved for those variables and the factor of safety is found in that fashion.

19.9.4 Critical Failure Circle

The method of slices gives the factor of safety for a chosen failure circle. The trick is to find which circle will give the lowest possible factor of safety; this is called the *critical circle*. Because the center of the circle and the radius of the circle can both vary, there is a double infinity of possible circles. The search for the critical circle typically proceeds by choosing a center location and then varying the radius of the circle until the lowest factor of safety is found for that center. That center is then assigned the corresponding value of the factor of safety. Many different centers are tried and each time the radius is varied until the minimum factor of safety is found for that center. A map is prepared of the center locations and the associated factors of safety (Figure 19.26). This map describes the surface of the factor of safety F in two dimensions ($F = F(x, y)$).

Two options are available for a computer program to search for the minimum factor of safety: the automatic search and the grid approach. Some software programs have an automatic search mode, in which the slope of the surface F(x,y) is used to move the location of the center toward lower F values until a minimum is found. The problem with this approach is that the minimum could be a local minimum and not the absolute minimum. This is a bit like finding a low valley in a mountain range but not finding the deepest valley over the peak next to it. One way to alleviate this problem is to repeat the automatic search by starting the search at a different center location.

With the grid approach, the user inputs a grid of center locations and the program outputs the factor of safety surface, leaving the decision of where the minimum factor of safety might be up to the user. A broad grid is used at first and can be refined once the likely location is more precisely identified.

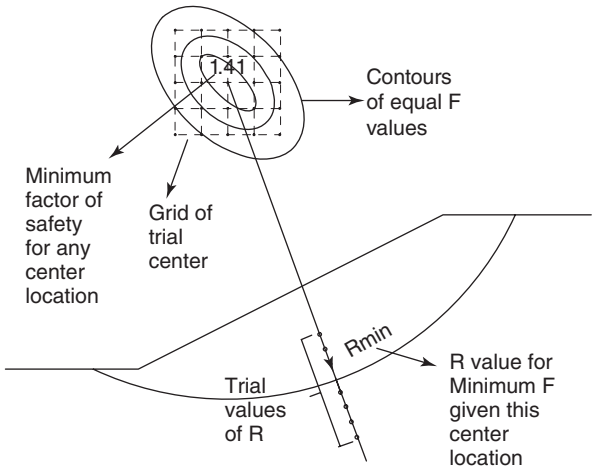

Figure 19.26 Finding the location of the minimum factor of safety.

19.10 WATER STRESS FOR SLOPE STABILITY

The water stress along the bottom of the failure surface has a significant influence on the factor of safety. The water stress at the bottom of a slice can be positive (below the groundwater level) or negative (above the groundwater level). A high positive water stress (compression) leads to a low factor of safety, whereas a high negative water stress (tension) leads to a high factor of safety. There are several ways to estimate the water stress in a slope: piezometric surface, water stress ratio value r_u, and grid of water stress values (Figure 19.27).

19.10.1 Piezometric and Phreatic Surface

A distinction must be made between the groundwater level, also called the *phreatic surface*, and the piezometric surface. If you drill a borehole in the ground, water will come to equilibrium at a certain level in the hole: this level corresponds to the phreatic surface or groundwater level. If you consider a point M in the ground and calculate the water stress at M as the product of the unit weight of water times the distance from M to a surface, then that surface is the piezometric surface. The groundwater level does not depend on the location of M, but the piezometric surface does. In most cases the piezometric surface is slightly below the phreatic surface, and using the phreatic surface as the piezometric surface will lead to a factor of safety slightly lower than the true factor of safety. The expression of the water stress u_w at point M is then:

$$u_w = \gamma_w h_p \tag{19.97}$$

where γ_w is the unit weight of water and h_p is the pressure head (positive or negative). The *pressure head* is the vertical

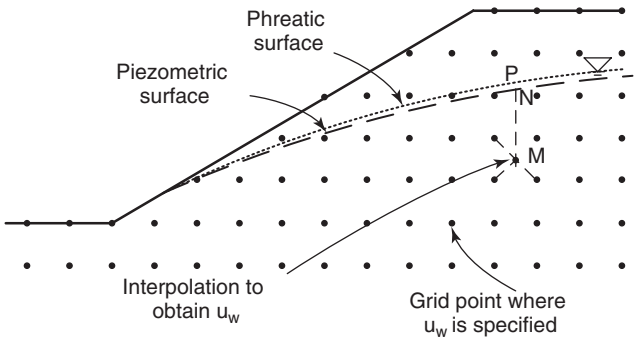

Figure 19.27 Input of water stress.

distance between point M and the piezometric surface. In the absence of a piezometric surface, the phreatic surface or groundwater level can be used as a first approximation. Note that if the point is above the groundwater level, the water stress will be negative, indicating water tension.

19.10.2 Water Stress Ratio Value

The water stress ratio r_u is defined as:

$$r_u = \frac{u_w}{\sigma_{ov}} \tag{19.98}$$

where u_w is the water stress at a point M and σ_{ov} is the total vertical stress at the same point M. Specifying a single value of r_u *for* a slope is very convenient, as it becomes simple to calculate the water stress at the bottom of the slice from the total vertical stress at the bottom of the slice. The problem is that the true r_u value may vary from one location along the failure surface to another; thus, this is a simplification, albeit a convenient one. Using a single r_u value is cruder than using a piezometric or phreatic surface, particularly for points of the failure surface that are above the groundwater level.

19.10.3 Grid of Water Stress Values

The approach that uses a grid of water stress values consists of inputting the water stress in the slope mass at grid points canvassing the slope. This input solution is more time-consuming than the two previously mentioned solutions, but it is also the most precise and versatile way to input the water stress. The grid size can vary, but should be fine enough that the interpolation between grid points leads to reasonable accuracy in the value of the water stress (Figure 19.27). Note that negative values (water tension) can be input with this solution at appropriate places in the grid.

19.10.4 Water Stress Due to Loading

If the slope is subjected to loading that induces water stress, the approach consists of calculating the hydrostatic water stress and the excess water stress separately:

$$u_w = u_{wo} + \Delta u_{we} \tag{19.99}$$

where u_{wo} is the hydrostatic component and Δu_{we} is the excess water stress. If the excess water stress is due to loading on the ground surface, it is generally calculated by first calculating the vertical normal total stress increase due to the load $\Delta\sigma_v$ in the soil mass (see section 17.8.7). Then the value of Δu_{we} is related to $\Delta\sigma_v$ by:

$$\overline{B} = \frac{\Delta u_{we}}{\Delta\sigma_v} \tag{19.100}$$

The value of the water stress parameter $\overline{B}$ is 1 in soft, saturated soil under the water table, but can be much smaller in stiff, overconsolidated soils. If $\overline{B}$ is not known, one solution is to assume a value (0.5, for example), calculate the factor of safety with that assumption, monitor the water stress in the slope with piezometers during construction, and stop construction if the water stress goes over the assumed value if that value is critical. One particular case in which such an approach is warranted is when an embankment is built over a soft clay.

19.10.5 Seepage Analysis

If water seeps through a slope, the water stress will be different from hydrostatic conditions. To calculate the water stress in this case, a flow net solution can be used (see sections 13.2.12 to 13.2.16). Figure 19.28 shows an example. In this case, the water stress at point M is given by equation 19.97, where h_p is the pressure head expressed as:

$$h_p = h_t - h_e \tag{19.101}$$

where h_t and h_e are the total head and elevation head at M respectively. Referring to Figure 19.28, the total head at M is the same as the total head at A, because they are on the same equipotential line. Because the pressure head at A is zero, the pressure head at M is expressed as follows:

$$h_{tM} = h_{tA} \quad and \quad h_{pA} = 0 \quad then \quad h_{pM} = h_{eA} - h_{eM} \tag{19.102}$$

and the pressure head at M is the difference in elevation between M and A. Thus, the piezometric line is slightly below the phreatic line. If the slope is relatively flat, as most soil slopes are, the difference is small, but if the slope is steep, the difference can be larger and using the phreatic line as the piezometric line can be excessively conservative.

19.11 TYPES OF ANALYSES

Several types of analyses can be performed, including:

1. Drained or undrained analysis
2. Effective stress or total stress analysis
3. Long-term or short-term analysis

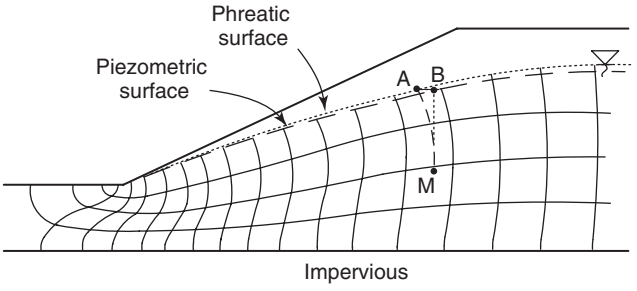

Figure 19.28 Flow net for slope stability.

In a *drained analysis*, the water stress is considered to be hydrostatic throughout the mass. The soil strength parameters associated with this analysis are the drained strength parameters or effective stress parameters.

An *undrained analysis* is used when the water does not have time to drain away. The soil strength parameter used in this case is the undrained shear strength. One must be careful to use the undrained shear strength corresponding to the stress path of the soil in the slope.

An *effective stress analysis* can be used in all cases. It makes no particular assumption regarding drainage and is based on sound fundamental principles. It makes use of the effective stress equation to obtain the shear strength of the soil based on the effective stress cohesion c' and the effective stress friction angle φ'. It can be used for an undrained analysis, a drained analysis, a short-term analysis, or a long-term analysis. The difficulty with using an effective stress analysis is that the water stress in the soil mass must be known. This is particularly challenging in the case of an undrained analysis.

A *total stress analysis* considers that the soil is made of one material; it does not recognize the existence of the three components (particles, water, and air). Hence, one must be very careful when using such an analysis. A total stress analysis can be used in the case of a soil with no water and in the case of a soil where the shear strength is independent of rapid variations in total stress. One such case is the undrained behavior of soft, compressible, saturated soils under the water table right after loading by an embankment.

A *long-term analysis* considers that all water stresses induced by loading have had time to dissipate and are back to hydrostatic. In this regard, a long-term analysis is similar to a drained analysis.

A *short-term analysis* is used for a soil condition taking place shortly after loading. As such, it is often a drained analysis for fast-draining soils like free-draining sands and gravels, and an undrained analysis for slow-draining soils like silts and clays.

The effective stress analysis is the preferred analysis, but it is also often the most difficult to perform, because of the complexities associated with predicting water stresses in the soil mass due to loading and due to desaturation close to the ground surface. In all cases it is wise to perform both a short-term and a long-term analysis for any soil problem to ensure proper behavior in the short and long terms.

19.12 PROGRESSIVE FAILURE IN STRAIN-SOFTENING SOILS

An added complexity in selecting the shear strength to use in the failure analysis occurs when the soil exhibits strain-softening behavior. In this case there is a peak strength τ_{fmax} and a residual strength τ_{fres} after the peak (Figure 19.29). The complexity comes from the fact that the failing body is not rigid and moves differently along the failure surface. The largest displacements along the failure surface typically start at the bottom of the slope and move back until they reach the top of the slope. Therefore, the displacement could be large enough to be at the residual shear strength toward the bottom of the slope but still be at the peak shear strength toward the top of the slope. This is called *progressive failure* (Figure 19.29). In the case of progressive failure, the back-calculated shear strength from a slope failure could be between the peak shear strength and the residual shear strength. Progressive failure is most likely to occur for slopes excavated in overconsolidated, stiff, fine-grained soils; such slopes may exist for several years before failing.

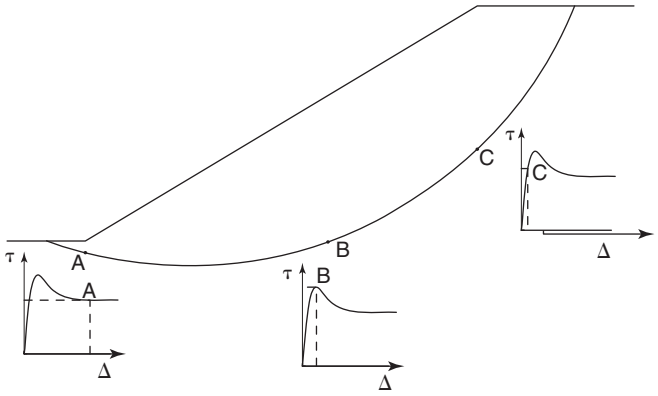

Figure 19.29 Progressive failure.

19.13 SHALLOW SLIDE FAILURES IN COMPACTED UNSATURATED EMBANKMENTS

Shallow slides may occur many years after an embankment is compacted at a water tension level that decreases with time, thereby weakening the soil strength. Aubeny and Lytton (2004) studied this problem and explained the phenomenon mathematically (see section 13.3.2) and experimentally. When embankments are built for freeway overpasses, for example, the approach embankment must be compacted and usually reaches a height of about 8 m. The side slopes are typically between 2 horizontal to 1 vertical and 3 horizontal to 1 vertical. The compaction takes place around the optimum water content (see Chapter 20), which corresponds to an unsaturated soil condition. Long after construction (e.g., 10 to 20 years), these embankments can experience shallow slide failures (Figure 19.30). The depth of these slides is about 1.5 to 2 meters. These failures take place because the water tension decreases as a function of time, as the as-built water tension is slowly reduced by repeated rainfalls. The drying and wetting process creates cracks that are typically as deep as they are horizontally spaced. This source of water at depth weakens the soil by decreasing the effective stress tied to the water tension—and the shallow slope fails.

Figure 19.30 Shallow slide in a compacted embankment. (Courtesy of Professor Charles Aubeny, Texas A&M University.)

The parts of the world where the rainfall and the temperature vary a lot during the seasons (tropics) are most likely to experience this problem. The solution is either to perform the slope stability analysis by using a wetted shear strength of the compacted soil or to prevent the water tension from being lost as a function of time. Geosynthetic covers may achieve this result.

19.14 REINFORCED SLOPES

19.14.1 Reinforcement Type

Many types of reinforcements can be used in a slope (Figure 19.31). They include rigid steel inclusions, geosynthetics, soil nails, stone columns, tieback anchors, and piles. Among these types of reinforcements, only tieback anchors are posttensioned to a preset tension force; all others are not. Of course, in most cases, the reinforcement ends up being in tension under working load conditions. Some reinforcement is considered to be rigid (e.g., soil nails), whereas other reinforcement is considered to be flexible (e.g., geosynthetics). This rigidity has an impact on the moment arm associated with the reinforcement.

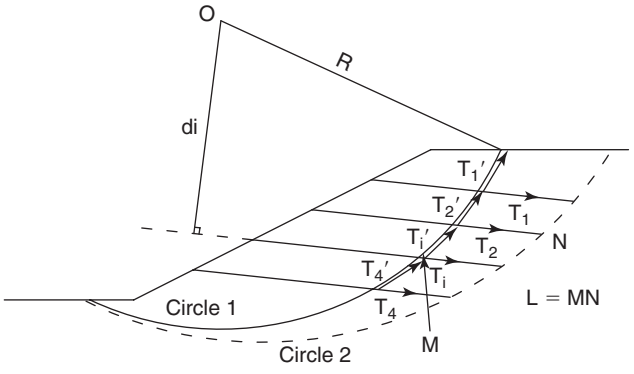

Figure 19.31 Reinforced slope.

19.14.2 Factor of Safety

The factor of safety for a slope and for a circular failure surface is defined in Eq. 19.81 as the ratio of the maximum resisting moment divided by the driving moment. Each layer of reinforcement increases the maximum resisting moment, so the factor of safety for a reinforced slope F_R is:

$$F_{\mathrm{R}} = \frac{M_{R\,\max(\mathrm{soil})} + M_{R\,\max(\mathrm{reinforcement})}}{M_D} \tag{19.103}$$

where $M_{R\,\max(\mathrm{soil})}$ is the maximum resisting moment provided by the soil along the failure circle considered, $M_{R\,\max(\mathrm{reinforcement})}$ is the maximum resisting moment provided by the reinforcement, and M_D is the driving moment due to the soil weight and any other external loads. For an unreinforced slope, the factor of safety $F_{\mathrm{unreinforced}}$ is:

$$F_{\mathrm{U}} = \frac{M_{R\,\max(\mathrm{soil})}}{M_D} \tag{19.104}$$

The expression of the maximum resisting moment provided by the reinforcement is:

$$M_{R\,\max(\mathrm{reinforcement})} = \sum_{i=1}^{n} T_i d_i \tag{19.105}$$

where T_i is the maximum resistance of the i^{th} reinforcement outside of the circle considered and d_i is the moment arm of the force T_i. The value of d_i depends on the flexibility of the reinforcement. If the reinforcement is rigid, such as soil nails, then the reinforcement will not bend along the potential plane of failure and the moment arm is the one associated with the direction of the reinforcement (d_i in Figure 19.31). If the reinforcement is flexible, then it will bend at the failure plane and follow the direction of the circle; in this case the moment arm of the reinforcement is the radius of the circle. The resistance force T_i is given by:

$$T_i = A_f f_u \tag{19.106}$$

where A_f is the contact area between the soil and the reinforcement (πDL for a cylindrical shape, 2(B + W)L for a rectangular shape), and f_u is the maximum shear stress that can be developed at the soil-reinforcement interface. The length L involved in calculating T_i is the length of reinforcement outside of the circle considered (MN in Figure 19.31). Note that for posttensioned reinforcement such as tieback anchors, the force T_i increases the compressive stresses on the failure plane, thereby increasing the shear strength along the plane of failure (see Chapter 21).

Another mode of failure in the case of a reinforced slope is for the failure circle to pass behind the reinforced zone (circle 2 in Figure 19.31). This circle is associated with a factor of safety F_2 (Eq. 19.104) which should be compared to F_1 of the reinforced slope (Eq. 19.103).

19.15 PROBABILISTIC APPROACH

In foundation engineering, uncertainty is included in the design through the use of load and resistance factor design (LRFD). In slope stability, LRFD is rarely used, but uncertainty does exist. The uncertainty associated with the calculated factor of safety in slope stability is quantified through a direct probability of failure calculation. This probabilistic approach has a great advantage over the deterministic approach, which gives only one value of the factor of safety. Imagine the following situations. You are given an average factor of safety equal to 1.5 and you feel comfortable about the safety of that slope. Then a probabilistic analysis is conducted to assess the probability of failure associated with the 1.5 factor of safety and yields a 0.2 or 1 chance in 5 of a failure occurring. Now you are not so comfortable about the 1.5 value. In contrast, if the assessed probability of failure turns out to be 0.001, you are very comfortable, as such a low probability of failure is well within the acceptable range for common civil engineering projects.

A background on probability is presented in section 11.6.1. The procedure for obtaining the probability of failure is outlined in section 11.6.2. A sample calculation of the probability of failure for a slope is given in section 11.6.4. The following simple examples illustrate the calculations to obtain the probability of failure.

19.15.1 Example 1

A slope exists as shown in Figure 19.32. It is made of clay with a normally distributed undrained shear strength s_u having a mean of 70 kPa and a standard deviation of 20 kPa. The failure circle has a radius of 16 m and the length of the arc is 24 m. The weight of the soil mass within the circle is 3200 kN per meter of length perpendicular to the page and the horizontal distance between the center of the circle and the center of gravity of the soil mass is 5.5 m.

The deterministic value of the factor of safety is:

$$F = \frac{RL}{Wa}s_u = \frac{16 \times 24}{3200 \times 5.5}70 = 1.527 \qquad (19.107)$$

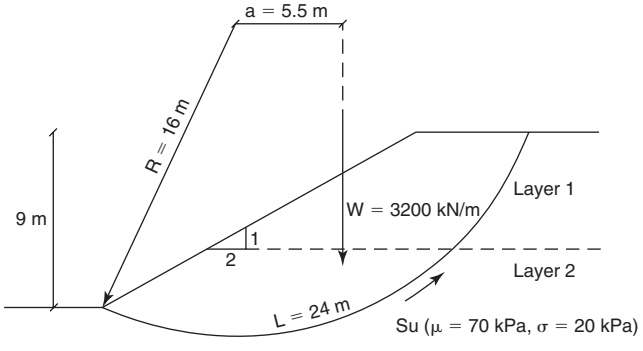

Figure 19.32 Probabilistic slope calculations example.

Note that if:

$$Y = aX \quad \text{then} \quad \mu_Y = a\mu_X \qquad (19.108)$$

Therefore, the value of the factor of safety in Eq. 19.107 is also the mean of F, μ_F. Let's calculate the standard deviation of F. Again we note that if:

$$Y = aX \quad \text{then} \quad \sigma_Y = a\sigma_X \qquad (19.109)$$

Therefore, the standard deviation of F is:

$$\sigma_F = \frac{RL}{Wa}\sigma_{s_u} = \frac{16 \times 24}{3200 \times 5.5} \times 20 = 0.436 \qquad (19.110)$$

Failure occurs when $F < 1$ and the probability that $F < 1$ is $P(F < 1)$, which can be evaluated as follows. The first step is to transform F into the standard normal variable U:

$$U = \frac{F - \mu_F}{\sigma_F} = \frac{F - 1.527}{0.436} \qquad (19.111)$$

The standard normal variable U has the following properties (see section 11.6.1):

$$P(U < u) = 1 - P(U < -u) \quad \text{and } P(U < u) = P(U > -u) \qquad (19.112)$$

We are looking for the probability:

$$P(F < 1) = P\left(\frac{F - \mu_F}{\sigma_F} < \frac{1 - 1.527}{0.436}\right) = P(U < -1.21) = 1 - P(U < 1.21) \qquad (19.113)$$

Table 11.3 gives:

$$P(U < 1.21) = 0.8869 \qquad (19.114)$$

and the probability of failure for this case is:

$$P(F < 1) = 1 - 0.8869 = 0.1131 \qquad (19.115)$$

For most civil engineering works, this would not be an acceptable probability of failure but the deterministic value of the factor of safety (1.527) would be.

19.15.2 Example 2

Consider the same slope geometry and the same circle, but now with the soil made of two layers. The top layer (crust) has a mean s_u value of 150 kPa, a standard deviation of 30 kPa, and a failure circle arc length of 6.5 m. The bottom layer has a mean s_u value of 70 kPa, a standard deviation of 20 kPa, and a failure circle arc length of 17.5 m. The weight and center of gravity of the soil mass are unchanged, with a weight of 3200 kN/m and a moment arm of 5.5 m.

The deterministic value of the factor of safety is:

$$F = \frac{R(L_1 s_{u1} + L_2 s_{u2})}{Wa} = \frac{16(6.5 \times 150 + 17.5 \times 70)}{3200 \times 5.5} = 2.0 \tag{19.116}$$

Note that if:

$$Y = aX + bZ \quad \text{then} \quad \mu_Y = a\mu_X + b\mu_Z \tag{19.117}$$

Therefore, the value of the factor of safety in Eq. 19.116 is also the mean of F, μ_F. It makes sense that the factor of safety would be higher than in Example 1, because we have replaced part of the soil with a stronger layer. Let's calculate the standard deviation of F. Again we note that if:

$$Y = aX + bZ \quad \text{then} \quad \sigma_Y = \sqrt{a^2\sigma_X^2 + b^2\sigma_Z^2} \tag{19.118}$$

Therefore, the standard deviation of F is:

$$\sigma_F = \sqrt{\left(\frac{16 \times 6.5}{3200 \times 5.5}\right)^2 30^2 + \left(\frac{16 \times 17.5}{3200 \times 5.5}\right)^2 20^2} = 0.364 \tag{19.119}$$

We follow the same process as in Example 1:

$$U = \frac{F - \mu_F}{\sigma_F} = \frac{F - 2.0}{0.364} \tag{19.120}$$

Then, we are looking for the probability:

$$P(F < 1) = P\left(\frac{F - \mu_F}{\sigma_F} < \frac{1 - 2.0}{0.364}\right) = P(U < -2.747) = 1 - P(U < 2.747) \tag{19.121}$$

Table 11.3 gives:

$$P(U < 2.747) = 0.997 \tag{19.122}$$

and the probability of failure for this case is:

$$P(F < 1) = 1 - 0.997 = 0.003 \tag{19.123}$$

This is an acceptable probability of failure in civil engineering. The main reason why the probability of failure has dramatically decreased (from 0.113 to 0.003) is that the mean factor of safety (2 instead of 1.527) is now further away from the failure value ($F = 1$).

19.15.3 Example 3

Let's repeat Example 1, but with two layers as in Example 2, except that these two layers are now identical and made of the Example 1 soil: mean $s_u = 70$ kPa and standard deviation of $s_u = 20$ kPa. The new calculations are as follows.

The deterministic value of the factor of safety is:

$$F = \frac{R(L_1 s_{u1} + L_2 s_{u1})}{Wa} = \frac{16(6.5 \times 70 + 17.5 \times 70)}{3200 \times 5.5} = 1.527 \tag{19.124}$$

It makes sense that we find the same factor of safety as in Example 1. The standard deviation of F has changed, however; it is now:

$$\sigma_F = \sqrt{\left(\frac{16 \times 6.5}{3200 \times 5.5}\right)^2 20^2 + \left(\frac{16 \times 17.5}{3200 \times 5.5}\right)^2 20^2} = 0.339 \tag{19.125}$$

We follow the same process as in Example 1:

$$U = \frac{F - \mu_F}{\sigma_F} = \frac{F - 1.527}{0.339} \tag{19.126}$$

Then, we are looking for the probability:

$$P(F < 1) = P\left(\frac{F - \mu_F}{\sigma_F} < \frac{1 - 1.527}{0.339}\right) = P(U < -1.555) = 1 - P(U < 1.555) \tag{19.127}$$

Table 11.3 gives:

$$P(U < 1.555) = 0.9400 \tag{19.128}$$

and the probability of failure for this case is:

$$P(F < 1) = 1 - 0.940 = 0.060 \tag{19.129}$$

This is about half the probability of failure calculated in Example 1, yet the soil conditions are the same except that we divided the soil into two identical layers. The reason for the decrease in the probability of failure is that if you randomly select a shear strength value from two identical distributions, you are very likely to make errors that tend to balance each other or reduce the error. The reason for this balancing error is that if you randomly pick a value that is too high for the first layer, you are more likely to pick a value that is too low for the second layer, as there are more values lower than your first guess. If there is only one layer, you have only your first guess for the calculations.

19.16 THREE-DIMENSIONAL CIRCULAR FAILURE ANALYSIS

The analysis of the circular failure in the preceding sections has assumed a plane strain condition. This means that the failing soil body has the shape of a cylindrical sector. Although in most cases this is a reasonable approximation, slope failures are always three dimensional (Figure 19.33). Three-dimensional or 3D slope failure analyses can be performed,

Figure 19.33 Three-dimensional slope failure. (Courtesy of Gordon W. Hunter, British Columbia Ministry of Transportation and Infrastructure.)

but are not done as commonly as plane strain analyses. One reason is that, most of the time, the assumption of a plane strain condition leads to a conservative factor of safety.

One way to perform a 3D slope stability analysis is to decompose the soil volume into a series of slices, each of which is considered to be a plane strain case (Figure 19.34). Many different assumptions can be made for such a mechanism, as was done for the 2D case. Some of them include a common axis of rotation for all circles and no forces between the circle slices. It can be seen in Figure 19.34 that if the deepest circle in the center of the volume is the critical circle for the 2D case, then all other circles will have a factor of safety higher than the 2D critical circle. From this observation, it follows that the global factor of safety for the 3D volume will be higher than for the 2D case. Though there are some exceptions to this statement, it is the general trend and has been documented

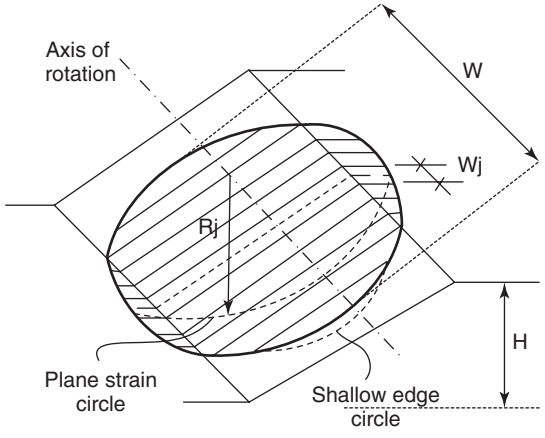

Figure 19.34 Decomposition of a 3D soil body into 2D soil slices.

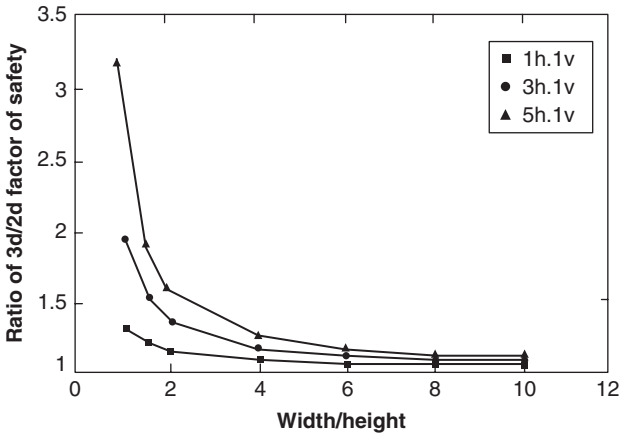

Figure 19.35 Comparison of 3D to 2D factor of safety. (After Stark 2003.)

by Stark (2003), for example (Figure 19.35). In Figure 19.35, H is the height of the slope and W is the width of slope considered in the analysis (sum of w_j on Figure 19.34). Three curves are shown for three different slope angles (1h to 1v, 3h to 1v, and 5h to 1v).

For the 2D case, the factor of safety of the j^{th} circle (Bishop simplified) is modified after Eq. 19.91:

$$F_{2D,j} = \frac{\sum_{i=1}^{n} \frac{1}{m_{\theta ij}} (c'_{ij} b_{ij} + (W_{ij} - \alpha_{ij} u_{wij} b_{ij}) \tan \varphi'_{ij})}{\sum_{i=1}^{n} W_{ij} \sin \theta_{ij}} \tag{19.130}$$

where all parameters are defined in Table 19.1 and j is the number of the circle slice as shown in Figure 19.34. Then, if the axis of rotation is the same for all slices and if the forces between the circle slices are neglected, the factor of safety for the 3D volume becomes:

$$F_{3D} = \frac{\sum_{j=1}^{m} R_j w_j \sum_{i=1}^{n} \frac{1}{m_{\theta ij}} (c'_{ij} b_{ij} + (W_{ij} - \alpha_{ij} u_{wij} b_{ij}) \tan \varphi'_{ij})}{\sum_{j=1}^{m} R_j w_j \sum_{i=1}^{n} W_{ij} \sin \theta_{ij}} \tag{19.131}$$

where R_j and w_j are the radius and width of the circle slice j respectively.

The drastic assumptions associated with this equation limit its applicability to a first estimate. A number of computer programs are available to perform more sophisticated 3D analyses. The goal of the assumptions, as in the 2D case, is to make the problem a statically determinate problem and to satisfy equilibrium equations in all directions. In the end, the finite element method is again the best way to solve the 3D problem, because with this method all equilibrium equations will automatically be satisfied for all elements of soil.

19.17 FINITE ELEMENT ANALYSIS

The finite element method (FEM) can be used to analyze the stability of slopes. The mesh should be large enough that the boundaries have only a small and tolerable influence on the stability calculations. If the height of the slope is H, the mesh should be at least 3 H high. If the horizontal distance between the toe and the crest of the slope is L, the mesh should be at least 5 L long. The advantages of the FEM over the limit equilibrium method (LEM) are that (Griffiths and Lane 1999):

1. No assumptions need be made about the failure surface; the weakest surface will automatically be found through the stress field calculated as part of the solution.
2. All equilibrium equations are satisfied.
3. In addition to a factor of safety, information is obtained on the displacements of the slope. This information, of course, is only as good as the soil model and soil properties used to obtain it.
4. The FEM includes complex issues such as progressive failure up to complete failure.

The factor of safety is determined through the use of a strength reduction factor (SRF) which is applied to the strength parameters of the soil:

$$c'_r = \frac{c'}{SRF} \tag{19.132}$$

$$\tan \varphi'_r = \frac{\tan \varphi'}{SRF} \tag{19.133}$$

where c' and φ' are the effective stress cohesion and friction angle of the soil respectively, and c'_r and φ'_r are the reduced effective stress cohesion and friction angle of the soil respectively. The FEM is performed repeatedly as the values of c'_r and φ'_r are gradually decreased by using an increasing SRF. The failure criterion can be defined in various ways (Abramson et al. 2002):

1. Bulging of the slope surface
2. Limiting shear stress reached on the failure surface
3. Nonconvergence of the solution

When an agreed-upon failure criterion is reached, the SRF is equal to the safety factor. Figure 19.36 shows an FEM output of a failed slope.

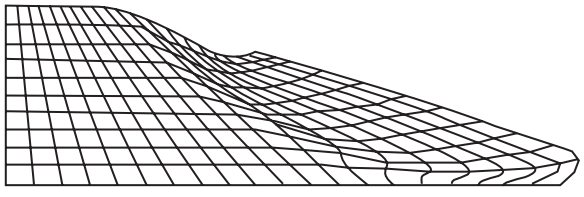

Figure 19.36 Failed slope in finite element method. (Courtesy of Griffiths and Lane 1999.)

19.18 SEISMIC SLOPE ANALYSIS

An earthquake can induce failure of a slope that is statically safe. The reason is twofold: The earthquake increases the driving moment, mostly through horizontal shaking; and in some soils it can decrease the shear strength of the soil by increasing the water compression stress through cyclic loading, possibly leading to liquefaction. There are several ways to include earthquake loading in slope stability analysis:

1. Pseudostatic method
2. Newmark's displacement method
3. Postearthquake stability method
4. Dynamic finite element method

19.18.1 Pseudostatic Method

The *pseudostatic method* is the most common and the simplest. It consists of adding a horizontal and vertical static force in the limit equilibrium analysis. These two forces are chosen to be equivalent to the effects of the inertia dynamic forces generated during shaking of the soil mass. They are assumed to be proportional to the weight W of the failing soil mass. The coefficients of proportionality are k_h and k_v for the horizontal and vertical direction respectively (Figure 19.37). Most commonly, the vertical seismic coefficient k_v is assumed to be zero and the horizontal seismic coefficient k_h depends on the severity of the shaking. Table 19.6 (Abramson

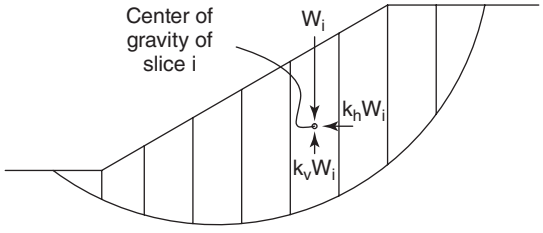

Figure 19.37 Pseudostatic seismic forces.

Table 19.6 Values of the Seismic Horizontal Coefficient k_h

Seismic Coefficient k_h	Comment
0.10	Major earthquake, U.S. Army Corps of Engineers, 1982
0.15	Great earthquake, U.S. Army Corps of Engineers, 1982
0.05 to 0.15	State of California
0.15 to 0.25	Japan
1/3 to 1/2 of peak ground acceleration (PGA)	Marcuson and Franklin 1983

(After Abramson et al. 2002.)

et al. 2002) is a summary of some common values for the seismic coefficient k_h.

The seismic force is usually placed at the center of gravity of the slice. Seismic analyses indicate that most of the time, the peak acceleration increases as the wave propagates from the bottom to the top of the slope. This would mean that the point of application of the seismic force should be above the center of gravity of the slice (CG); this would generate smaller overturning moments than if that force were placed at the CG. Therefore, placing the seismic force at the CG of the slices, as is usual practice, is conservative in most cases.

Another way to approach the problem is to find the horizontal seismic coefficient k_h that would lead to failure of the slope. This value of k_h, called the *yield horizontal seismic coefficient* k_y, corresponds to a factor of safety of 1 (Figure 19.38). Then the value of k_y can be compared to the peak ground acceleration (PGA) of the earthquake at the slope location. Abramson et al. (2002) suggest the observations in Table 19.7.

Note that a very important part of the pseudostatic analysis, as for any slope stability analysis, is to select the correct shear strength. The issue here is that the shear strength during shaking is likely to be reduced compared to the static case.

19.18.2 Newmark's Displacement Method

Newmark's displacement method is credited to Newmark (1965). Whereas most other slope stability methods aim at predicting the factor of safety, this method aims at predicting the accumulation of displacement of the slope during a series of acceleration cycles, as in an earthquake, for example.

The first step is to develop an acceleration history a(t) for the earthquake at the location of the slope (Figure 19.39). Then the yield acceleration a_y is found by using the pseudostatic method. The relationship between a_y and k_y is:

$$a_y = k_y g \tag{19.134}$$

where g is the acceleration due to gravity. Any acceleration above a_y will lead to movement as the slope fails during a short time increment (points B to D in Figure 19.39). By integration of the net acceleration $(a(t)-a_y)$ from B to D, the velocity of the soil mass is found (points B_1 to D_1 in Figure 19.39). Then the velocity decreases as the acceleration recedes below a_y and the shear strength slows the soil mass down (points D_1 to M_1 in Figure 19.39). By integrating the velocity from B_1 to M_1, the displacement of the slope mass is obtained (points B_2 to M_2 in Figure 19.39). At M_2, a permanent displacement has been accumulated; the displacement increases again when the acceleration exceeds the yield acceleration (point H in Figure 19.39). The process repeats itself until the earthquake is over. One of the key parts of this method is developing the acceleration history for the slope. This is discussed in Chapter 22.

Makdisi and Seed (1978) performed a parametric analysis using actual and hypothetical dams and embankments. Using the results, they simplified Newmark's method and presented it in the form of a chart (Figure 19.40). The acceleration ratio k_y/k_{max} is on the horizontal axis, where k_y is the yield horizontal seismic coefficient corresponding to failure of the slope and k_{max} is the maximum acceleration horizontal seismic coefficient corresponding to the maximum acceleration

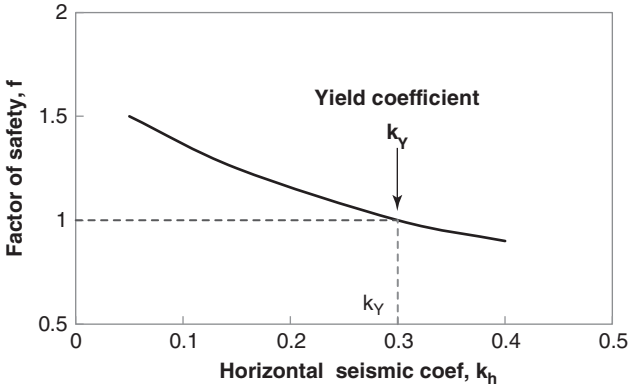

Figure 19.38 Yield horizontal seismic coefficient.

Table 19.7 Likelihood of Failure for Different Values of k_y

Relative Position of k_y and PGA	Observation
k_y > PGA	No failure likely
0.5 PGA < k_y < PGA	Minor damage possible
k_y < 0.5 PGA	Failure likely

(After Abramson et al. 2002.)

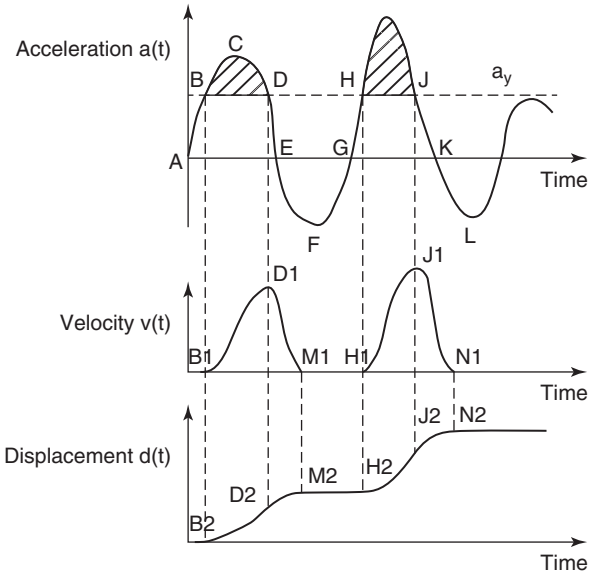

Figure 19.39 Newmark's displacement method (1965).

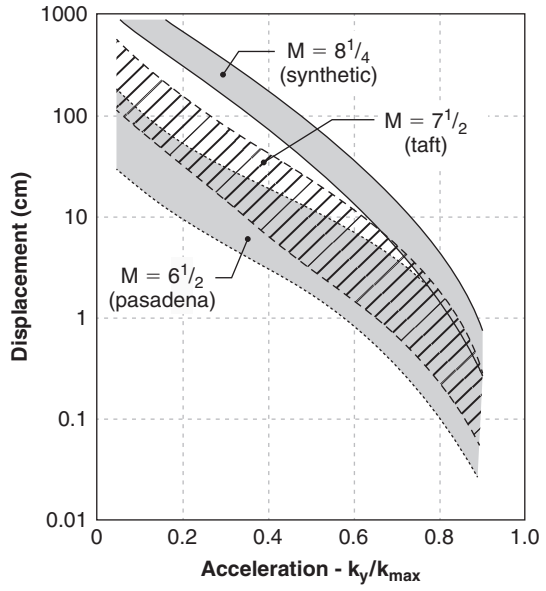

Figure 19.40 Makdisi and Seed (1978) chart. (This material is reproduced with permission of John Wiley & Sons, Inc.)

in the slope and defined as:

$$a_{max} = k_{max} g \tag{19.135}$$

The earthquake magnitude M (see Chapter 22) is selected for the site and the range of displacement is read on the vertical axis using the acceleration ratio and the magnitude M.

19.18.3 Postearthquake Stability Analysis

Postearthquake stability analysis is a static analysis that considers the situation right after an earthquake. The main issue in this case is the proper selection of the shear strength existing after the earthquake. The steps for such an analysis (Duncan and Wright 2005) include:

1. Study whether the soil has liquefied or not (see Chapter 22)
2. Determine the reduced shear strength due to cyclic loading (see Chapter 22)
3. Use that shear strength for a conventional stability analysis

19.18.4 Dynamic Finite Element Analysis

Dynamic finite element analysis is a 2D or 3D dynamic analysis of the slope and its surroundings. The finite element mesh should be large enough that the effect of the boundaries does not significantly affect the stability calculations for the slope. The recommendations of section 19.17 for static analysis may not be sufficient, as earthquake shaking creates waves that propagate against the boundaries and are reflected toward the slope. The soil model should incorporate the evolution of the strength and deformation properties as a function of cycles. The earthquake motion is usually induced at the bottom of the mesh and propagates upward through the slope mesh. The fact that the soil model can more closely follow the soil behavior and the fact that the dynamic equilibrium of the elements is satisfied at all times are two major advantages of this approach. The complexity of the approach is its drawback.

19.19 MONITORING

Monitoring consists of making observations or measurements on a slope in order to evaluate its stability. Among the most useful parameters to observe or measure are:

1. Cracks, particularly on top of the slope
2. Movements of the slope surface or at depth
3. Groundwater and water stress conditions

Crack openings are indications that a slope is stressed (Figure 19.41). Cracks associated with instability on top of slopes are parallel to the slope crest and are several meters long. If the cracks are less than 25 mm wide, and if there is no difference in elevation between the two sides, the probability of failure is low. If the cracks are between 25 and 75 mm wide, with some difference in elevation between the two sides, the probability of failure is much higher. If the cracks are much larger than 100 mm with similar difference in elevation between the two sides, it is likely time to run. Instruments to measure cracks can be as simple as a tape measure or as sophisticated as an extensometer that monitors the distance between the two sides and sends readings to a remote monitoring station. It is very useful to monitor crack width b as a function of time t and plot the curve b vs. t. If the growth rate of the crack opening decreases with time, it indicates a trend toward stability, but if the growth rate increases steadily with time, failure may be imminent. There are cases in which the growth rate decreases but then reverses to an increase with time (Figure 19.42).

Movements of the slope surface can be tracked with useful and simple measurements. Tools can be as simple as surveying stakes driven in the ground and as advanced as GPS monitoring. Movement of the crest is a good indication, but swelling or heaving at the base of the slope is also an early sign. As in the case of cracks, the shape of the curve of the movement as a function of time is the best indication of potential failure.

Movement at depth in the slope is a very useful but more complicated measure, and is expensive to obtain. The most common method is to place a vertical inclinometer casing through the surface of the slope to a depth well below the potential failure surface (Figure 19.43). The bottom of the slope indicator casing should be in a soil zone that is not influenced by the slope movement. The reason is that the bottom readings will represent the zero position for the casing. The slope inclinometer casing is grooved and the probe has wheels (Figure 19.44) that fit in the grooves to keep

(a)

(b)

(c)

(d)

Figure 19.41 Example of cracks on top of slopes. (*a*: From Bray et al. 2001. Used by permission. *b*: Photo by and courtesy of Jonathan Wilkins. c: Courtesy of Dr. Ian West.)

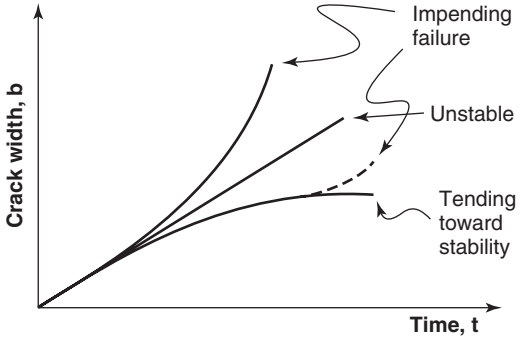

Figure 19.42 Monitoring crack width over time.

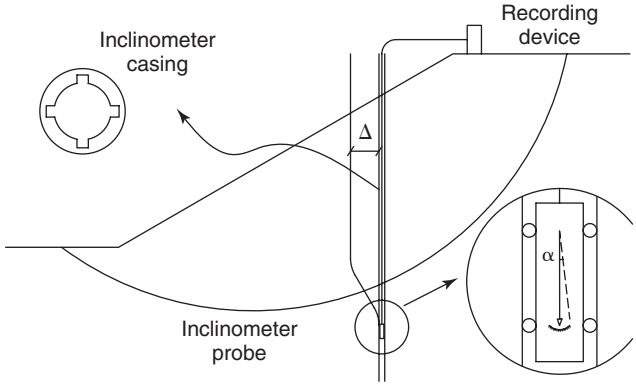

Figure 19.43 Inclinometer in a slope.

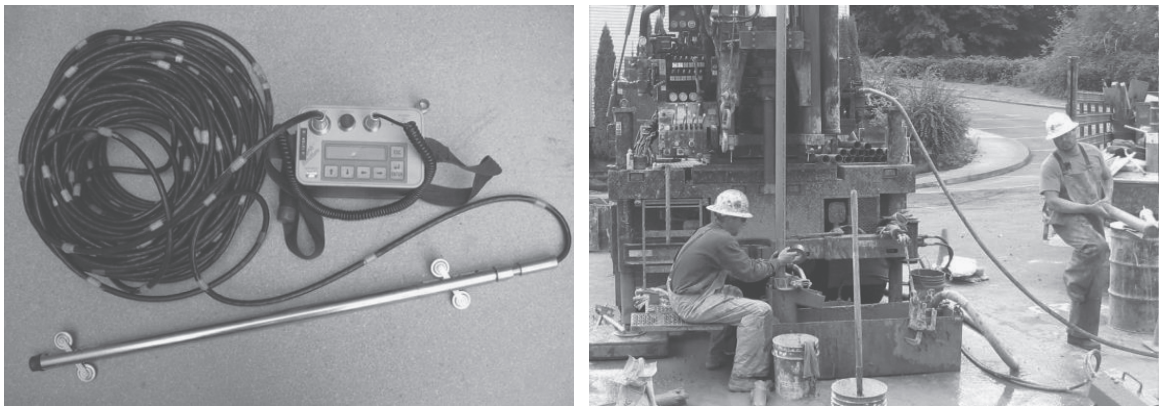

(a) (b)

Figure 19.44 Inclinometer instrument and casing installation. *(a)* Inclinometer. *(b)* Casing installation. (Courtesy of Landslide Technology.)

the direction of the probe constant during the readings. The probe is lowered to the bottom of the casing and then pulled up the casing while readings are taken at regular intervals. This interval is usually the length L of the probe between wheels (e.g., $L = 0.5$ m). The first reading R_1 is taken at the bottom of the casing at a depth z_1. The probe is pulled up an amount equal to L and the second reading R_2 at depth z_2 is obtained, and so on all the way to the top of the casing. The first set of readings in the casing is taken right after installation and provides a set of zero readings R_{oi}. It is assumed that the bottom of the casing is low enough below the slope potential failure surface that no movement takes place at the bottom of the casing; therefore, the readings at the bottom provide a reference for all the others. If there is doubt about whether the bottom is moving, then the top of the casing should be surveyed each time a set of inclinometer readings is taken.

Each reading represents the angle α between the probe direction and the vertical at that location. The instruments to measure this angle are servo-accelerometers located in the probe. A servo-accelerometer is essentially a mass placed at the end of a pendulum between two magnetic coils. When the pendulum begins to swing to a new position, a magnetic force is applied to keep the pendulum in the zero position. The current necessary for the magnetic force to keep the pendulum in the zero position is proportional to the angle that the pendulum would have taken had it not been restrained.

The reading R_i at depth z_i gives the angle of the inclinometer as:

$$\sin\theta_i = \frac{R_i}{C} \tag{19.136}$$

where C is a constant specific to each inclinometer and θ_i is the angle of the casing with the vertical at depth z_i.

Often readings will be taken in two opposite directions of the probe (0 and 180° in a horizontal plane) and the average of the two readings will be used. The horizontal distance d_i between the two points separating two consecutive readings (often the length between probe wheels) is given by (Figure 19.45):

$$d_i = L\sin\theta_i \tag{19.137}$$

where L is the increment of depth between readings. If the set of zero readings gave a value of d_i equal to d_{oi}, then the net horizontal distance is $(d_i - d_{oi})$. Because we want the overall position of the casing after deformation, it is necessary to add all net horizontal distances between all consecutive points from the bottom of the casing to the depth where the horizontal movement is required. If it is assumed that the

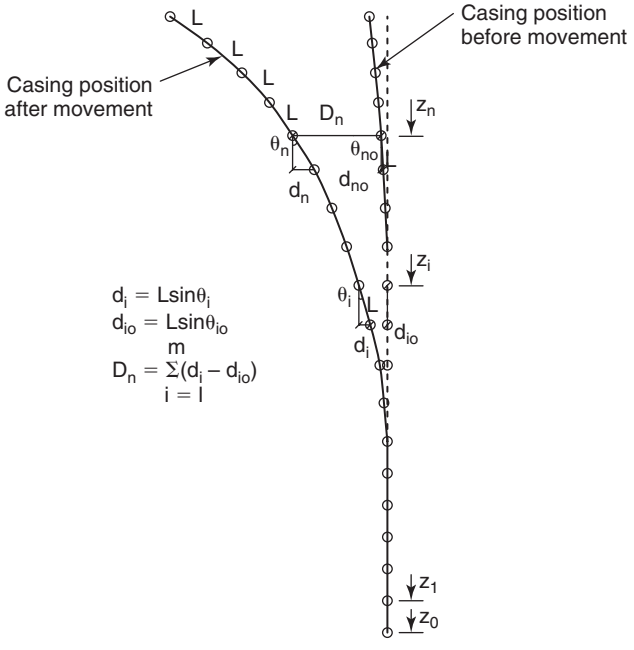

Figure 19.45 Inclinometer data reduction.

bottom of the casing is not moving, the horizontal movement of the casing at any depth z_n is (Figure 19.45):

$$D_n = \sum_{i=1}^{n}(d_i - d_{io}) = \frac{L}{C}\sum_{i=1}^{n}(R_i - R_{io}) \qquad (19.138)$$

Groundwater and water stress conditions are very important aspects of slope stability. The groundwater level can be measured by simply measuring the equilibrium water level in an open standpipe or by using a piezometer. If the water is in compression, the water stress can be measured with a piezometer. If the water is in tension, the water stress can be measured with a field tensiometer up to a water tension of −90 kPa. Above that value, a soil sample can be taken, the water content determined, and the soil water retention curve used to go from the water content to the water tension (see section 9.15).

19.20 REPAIR METHODS

There are essentially two ways to repair a slope that is getting close to failure (Figure 19.46):

1. Increase the resisting moment (e.g., soil improvement, inclusions)
2. Decrease the driving moment (e.g., shallower slope)

19.20.1 Increase the Resisting Moment

The shear strength s of the soil is:

$$s = c' + (\sigma - \alpha u_w)\tan\varphi' \qquad (19.139)$$

where c' is the effective stress cohesion intercept, σ is the normal total stress on the plane of failure, α is the area ratio for the water phase, u_w is the water stress, and φ' is the effective stress friction angle. Therefore, increasing s may consist of increasing c', or σ, or $\tan\varphi'$, or decreasing αu_w. Increasing c' can be done by chemical injection of cementing agents such as lime or cement. Increasing σ is usually not a good idea, as it also increases the driving moment. Increasing $\tan\varphi'$ is difficult, but can be done through densification by compaction or vibration. If the soil is saturated and if the water is in compression, the term αu_w becomes u_w and decreasing u_w consists of decreasing the water stress (through drainage, for example) if there are excess water stresses or by lowering the water level (by pumping, for example) if the water stress is hydrostatic. If the soil is saturated with water in tension or if the soil is unsaturated, decreasing u_w consists of drying or evaporation, for example. In this case u_w becomes more negative, but α also decreases, so the net result is not as efficient as a decrease in u_w alone. In some instances, the water tension is naturally decreased (less negative) during the life of the slope because of the weather. This may lead to failure, and one way to prevent such failures is to keep the water tension from changing by isolating the soil from the weather. Geosynthetic covers can achieve this goal.

The other way to increase the resisting moment is to insert inclusions in the slope and across the failure plane (Section 19.14). For existing slopes, soil nails or piles can be used. *Soil nails* are small-diameter inclusions that are placed most often by drilling and sometimes by driving. The drilling process consists of drilling a hole, removing the drilling tool, inserting a steel bar or cable with centralizers in the hole, and grouting the annulus between the bar and the soil. Soil nails have the advantage that they are relatively easy to place at any inclination, although they are most often placed nearly horizontally. Piles are placed vertically

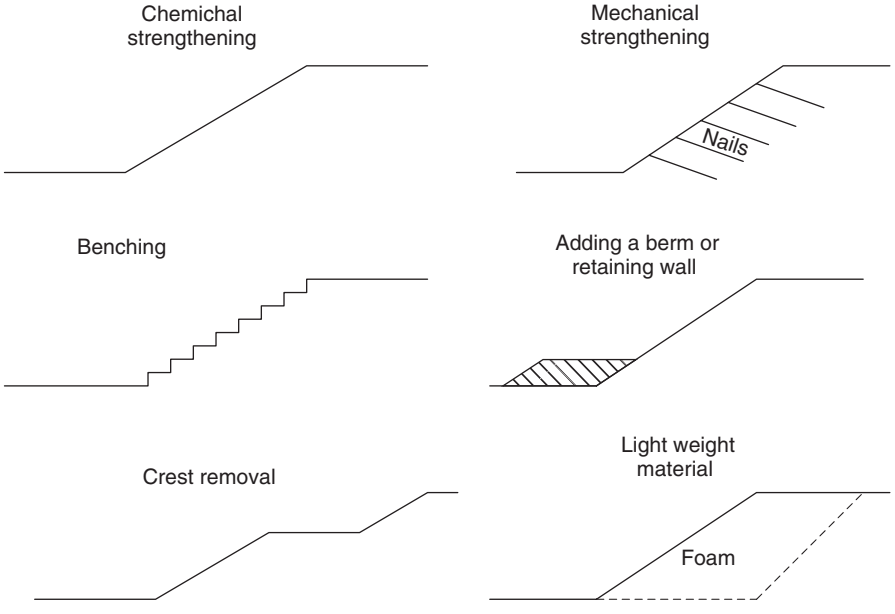

Figure 19.46 Slope repair methods.

or near vertically and have a larger diameter than nails. For new slopes like embankments, geosynthetic layers or reinforcing steel strips can be placed as reinforcement.

19.20.2 Decrease the Driving Moment

The driving moment M_d *for* the slope is:

$$M_d = Wa \tag{19.140}$$

where W is the weight of the failing soil mass and a is the horizontal distance from the center of the failure circle for a circular failure surface and the center of gravity of the failing soil mass. Therefore, decreasing M_d consists of decreasing W or a or both. To decrease W, lightweight material such as foam can be used for embankments. Also, the slope angle can be reduced by removing part of the crest, adding a berm at the bottom of the slope, or simply grading the slope to a flatter angle (Figure 19.46).

In the end, the choice of one method or another is based on effectiveness of the method, feasibility, and cost. For landfill slopes, see section 24.7.6. For slopes involving geosynthetics, see section 25.6.3.

PROBLEMS

19.1 Calculate the factor of safety for the slope shown in Figure 19.1s in the following cases:
- a. Slope alone
- b. Slope plus building
- c. Slope plus building and earthquake
- d. What is the yield coefficient k_y for that slope?

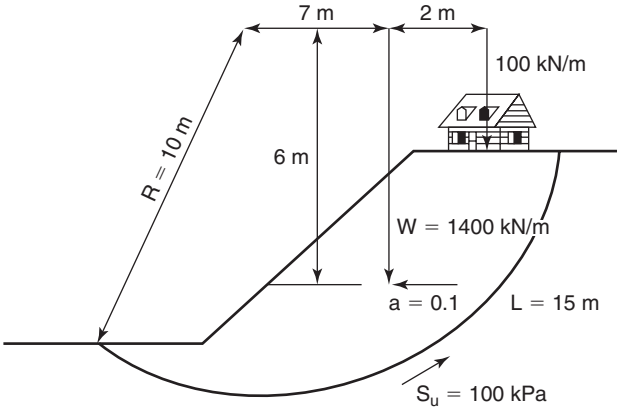

Figure 19.1s Slope with building and earthquake.

19.2 An infinite slope is made of sand with a friction angle of 32° and a unit weight of 20 kN/m^3. The slope angle is 2.5 horizontal to 1 vertical. Calculate the factor of safety in the summer when the slope has no water, then calculate the factor of safety in the spring when the slope is filled with water.

19.3 Derive the expression for the factor of safety of an infinite slope with a failure plane parallel to the ground surface at a depth h and with a groundwater level at a height mh above the failure plane ($m < 1$).

19.4 Design a safe slope angle for an excavated slope in a stiff clay to reach a 20 m deep deposit of lignite. The stiff clay has effective shear strength parameters of $c' = 10$ kPa and friction angle $\varphi' = 25°$. Consider the case where the water level is not within the slope failure zone and then the one where the water level follows the slope contour. Use the chart method. In practice, it is not uncommon to see such excavations with much steeper slopes than the answer you will get in this problem; although failures do occur, they do not occur too often. Why do you think that is?

19.5 Calculate the factor of safety by using Janbu's charts for the slope shown in Figure 19.2s in the following cases:
- a. Case 1 : $Hw = Hw' = 10$ m
- b. Case 2 : $Hw = 0$, $Hw' = 10$ m
- c. Case 3 : $Hw = Hw' = 0$

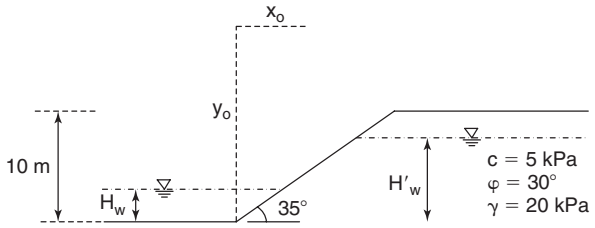

Figure 19.2s Slope with different water levels.

19.6 A 3 horizontal to 1 vertical slope is cut in a clay that has an effective stress cohesion of 5 kPa and an effective stress friction angle of 30°. The slope is 6 m high. Calculate:
   a. The factor of safety of the slope against long-term failure if the water table is below the critical circle.
   b. The factor of safety of the slope against long-term failure if the water table coincides with the slope contour.

19.7 Calculate the probability of failure of a slope that has a factor of safety with a mean of 1.5 and a coefficient of variation of 0.2 (assume that the factor of safety is normally distributed). If the acceptable probability of failure is 0.001, what must be the mean value of the factor of safety if the coefficient of variation remains equal to 0.2?

19.8 Which situation is more desirable? Explain and demonstrate.
   a. Mean factor of safety $F = 1.5$ and coefficient of variation of $F = 0.2$
   b. Mean factor of safety $F = 1.3$ and coefficient of variation of $F = 0.1$

19.9 Calculate the factor of safety for the slope shown in Figure 19.3s. Select your best estimate of the critical circle and calculate the factor of safety by the Bishop modified method of slices.

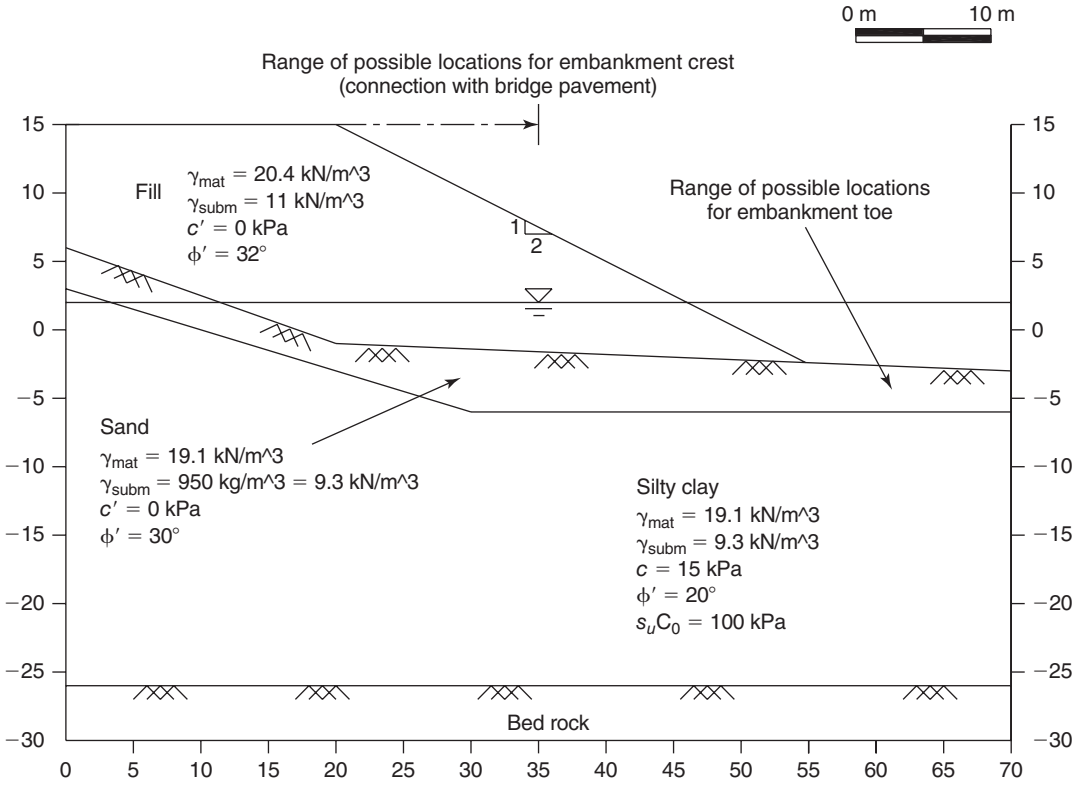

Figure 19.3s Slope of Fredericton embankment.

19.10 A slope is subjected to an acceleration history as shown in Figure 19.4s. The yield acceleration for that slope is 1.5 m/s^2. Calculate the displacement history of the slope according to Newmark's method.

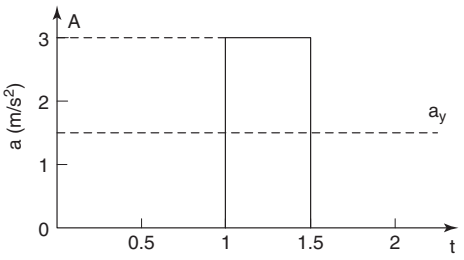

Figure 19.4s Acceleration history.

19.11 Consider the case of a $c' = 0, \varphi' > 0$ soil and demonstrate that for one slice, the factor of safety is the same for the ordinary method of slices (OMS) and for the Bishop simplified method of slices (BSMS). If it is true for one slice, why is it not true for n slices ($n > 1$)?

19.12 A 3D slope failure has a failure surface in the form of a sphere and a factor of safety F_{3D}. This sphere is sliced in a direction perpendicular to the crest. The slices have the same width b. The deepest slice in the center of the sphere has a factor of safety $F_{\min}$. Each slice has a 2D factor of safety equal to F_i. What other assumptions must be made for the following equation to be true? $F_{3D} = \frac{1}{n}\sum_{i=1}^{n} F_i$

19.13 A dry fine sand slope has a factor of safety of 1.5 on the Earth.
   a. Calculate and discuss the factor of safety for the same slope on the moon.
   b. Assume that there could be water on the moon. Would the result of the dry case still hold?

19.14 Define the seepage force and discuss when the seepage force should be considered in a slope stability analysis. Why is it not usually considered?

19.15 Explain the difference between the following analyses, including what shear strength you would use: total stress analysis, effective stress analysis, undrained analysis, drained analysis, short-term analysis, long-term analysis.

19.16 An inclinometer casing is attached to a 10 m high retaining wall. Zero readings taken before the wall is backfilled indicate that the wall is perfectly vertical. The backfill is placed and compacted. At the end of construction, the inclinometer readings are taken again. Find what the readings are if:
   a. The displacement y (m) of the wall obeys the equation $y = 0.01\ (z_{\max} - z)$ where $z_{\max}$ is the maximum depth the inclinometer probe can reach in the casing (10 m) and z is the depth at which the reading is taken.
   b. The displacement y (m) of the wall obeys the equation $y = 0.001\ (z_{\max} - z)^2$ where $z_{\max}$ is the maximum depth the inclinometer probe can reach in the casing (10 m) and z is the depth at which the reading is taken.

Problems and Solutions

Problem 19.1

Calculate the factor of safety for the slope shown in Figure 19.1s in the following cases:

a. Slope alone
b. Slope plus building
c. Slope plus building and earthquake
d. What is the yield coefficient k_y for that slope?

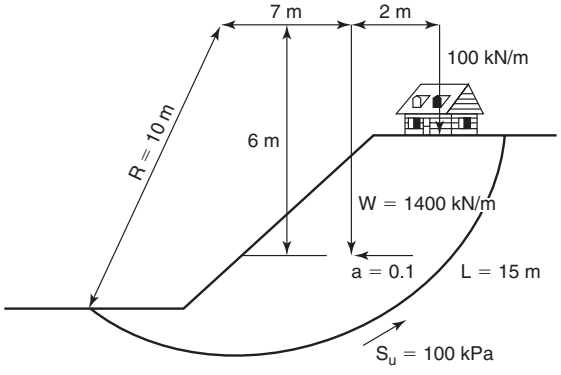

Figure 19.1s Slope with building and earthquake.

Solution 19.1

The factor of safety is the maximum resisting moment divided by the driving moment:

$$FS = \frac{Maximum\ resisting\ moment}{Driving\ Moment}$$

a. Slope alone:

$$FS = \frac{100 \times 15 \times 10}{1400 \times 7} = 1.53$$

b. Slope and building:

$$FS = \frac{100 \times 15 \times 10}{1400 \times 7 + 100 \times (7 + 2)} = 1.40$$

c. Slope plus building and earthquake:

$$FS = \frac{100 \times 15 \times 10}{1400 \times 7 + 100 \times (7 + 2) + 0.1 \times 1400 \times 6} = 1.30$$

d. The earthquake yield coefficient k_y for that slope:

$$FS = \frac{100 \times 10 \times 15}{1400 \times 7 + 100 \times (7 + 2) + k_Y \times 1400 \times 6} = 1.00 \ \Rightarrow \ k_Y = 0.51$$

Problem 19.2

An infinite slope is made of sand with a friction angle of 32° and a unit weight of 20 kN/m^3. The slope angle is 2.5 horizontal to 1 vertical. Calculate the factor of safety in the summer when the slope has no water, then calculate the factor of safety in the spring when the slope is filled with water.

Solution 19.2

For the case of sand with no water during the summer:

$$FS = \frac{\tan\varphi'}{\tan\beta} = \frac{\tan(32)}{1/2.5} = 1.56$$

For the case of the sand filled with water during the spring with no cohesion, and assuming a saturated unit weight of 22 kN/m^3 :

$$FS = \frac{(\gamma_{sat} - \gamma_w)}{\gamma_{sat}} \frac{\tan\varphi'}{\tan\beta} = \frac{(22 - 9.81)}{22} \frac{\tan(32)}{1/2.5} = 0.86$$

The presence of water significantly reduces the factor of safety of the slope.

Problem 19.3

Derive the expression for the factor of safety of an infinite slope with a failure plane parallel to the ground surface at a depth h and with a groundwater level at a height mh above the failure plane (m < 1).

Solution 19.3

Let's call γ_{m} the soil unit weight above the groundwater level and γ_{sat} the soil unit weight below the groundwater level. Referring to Figure 19.6 and the case of the infinite slope with seepage, the shear strength on the failure plane is:

$$\tau_f = c' + (\gamma_m(1 - m)h\cos^2\beta + \gamma_{sat}mh\cos^2\beta - \gamma_w mh\cos^2\beta)\tan\varphi'$$

$$\tau_f = c' + ((1 - m)\gamma_m + m(\gamma_{sat} - \gamma_w))h\cos^2\beta\tan\varphi'$$

The shear stress τ on the plane of failure is:

$$\tau = (\gamma_m(1-m)h\cos\beta + \gamma_{sat}mh\cos\beta)\sin\beta$$
$$\tau = ((1-m)\gamma_m + m\gamma_{sat})h\cos\beta\sin\beta$$

The factor of safety is:

$$FS = \frac{c' + ((1-m)\gamma_m + m(\gamma_{sat}-\gamma_w))h\cos^2\beta\tan\varphi'}{((1-m)\gamma_m + m\gamma_{sat})h\cos\beta\sin\beta}$$
$$FS = \frac{c'}{((1-m)\gamma_m + m\gamma_{sat})h\cos\beta\sin\beta} + \frac{((1-m)\gamma_m + m(\gamma_{sat}-\gamma_w))}{((1-m)\gamma_m + m\gamma_{sat})} \times \frac{\tan\varphi'}{\tan\beta}$$

Problem 19.4

Design a safe slope angle for an excavated slope in a stiff clay to reach a 20 m deep deposit of lignite. The stiff clay has effective shear strength parameters of $c' = 10$ kPa and friction angle $\varphi' = 25^\circ$. Consider the case where the water level is not within the slope failure zone and then the one where the water level follows the slope contour. Use the chart method. In practice, it is not uncommon to see such excavations with much steeper slopes than the answer you will get in this problem; although failures do occur, they do not occur too often. Why do you think that is?

Solution 19.4

If the soil is uniform and a circular failure surface is assumed, chart methods can be used.

a. Case of No Water

a-1. Taylor (1948) (Figure 19.5s)

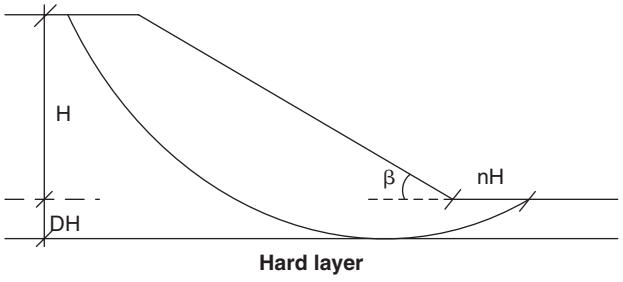

Figure 19.5s Sketch of problem 19.4.

Let's assume toe circles on Figure 19.13 with $c' = 10$ kPa, $\varphi' = 25^\circ$, and $\gamma = 20$ kN/m^3. We start with an assumed factor of safety where c' equals 1.5.

The developed friction angle is calculated using:

$$\varphi_d = \tan^{-1}\left(\frac{\tan\varphi}{FS}\right) = \tan^{-1}\left(\frac{\tan 25}{1.5}\right) = 17.26^\circ$$
$$F'_c = \frac{c'}{c'_d} \quad and \quad F_{\varphi'} = \frac{\tan\varphi'}{\tan\varphi'_d}$$
$$F'_c = \frac{c'}{c'_d} = 1.5 \rightarrow c'_d = \frac{10}{1.5} = 6.67 \text{ kPa}$$

The stability number $N = \dfrac{c'_d}{\gamma H} = \dfrac{6.67}{20\times 20} = 0.0167 \rightarrow$ Figure 19.13 $\rightarrow \beta = 22^\circ$

a-2. Spencer (1973)

$$r_u = \frac{u_w}{\sigma_{0v}} = 0 \quad \text{because there is no water}$$

$$F'_c = \frac{c'}{c'_d} \;\; and \;\; F_{\varphi'} = \frac{\tan\varphi'}{\tan\varphi'_d}$$

$$F'_c = \frac{c'}{c'_d} = 1.5 \rightarrow c'_d = \frac{10}{1.5} = 6.67 \text{ kPa} \quad \text{and} \quad N = \frac{c'_d}{\gamma H} = \frac{6.67}{20 \times 20} = 0.0167$$

Figure 19.15 $\rightarrow r_u = 0 \rightarrow \beta = 23^\circ$

b. Water Case

b-1. Taylor (1948), undrained: $s_u = 70$ kPa ($\varphi' = 0$)

Assuming a toe circle, a factor of safety of 1.5, and using $s_u = 70$ kPa:

$$FS = \frac{S_u}{c_d} \rightarrow c_d = \frac{S_u}{FS} = \frac{70}{1.5} = 46.67 \text{ kPa}$$

$$N = \frac{c_d}{\gamma H} = \frac{46.67}{20 \times 20} = 0.12 \rightarrow \text{Fig. 19.12 for n} = 0 \rightarrow \beta = 11^\circ$$

b-2. Spencer (1973), drained behavior: c', φ'

$$r_u = \frac{u_w}{\sigma_{0v}} = 0.5$$

Figure 19.15 $\rightarrow r_u = 0.5 \rightarrow \beta = 11^\circ$

Table 19.1s Slope Angle from Taylor and Spencer Methods

Slope Angle β	Taylor (1948)	Spencer (1973)
Dry case	22°	23°
Water case	11°	11°

Several factors come into play. First, the water in the soil is likely in tension, which increases the safe angle. Second, the excavation remains open for a limited amount of time and the soil behavior may be time dependent. The slopes may be well drained. The open-pit mine slope industry seems to accept a higher probability of slope failure as part of the economical optimization of the lignite mining process.

Problem 19.5

Calculate the factor of safety by using Janbu's charts for the slope shown in Figure 19.2s in the following cases:

a. Case 1 : $H_w = H'_w = 10$ m
b. Case 2 : $H_w = 0, H'_w = 10$ m
c. Case 3 : $H_w = H'_w = 0$

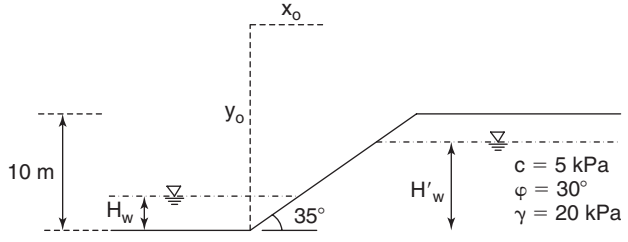

Figure 19.2s Slope with different water levels.

Solution 19.5

Janbu Chart

a. Case 1: $H_w = H'_w = 10$ m

$$\mu_w = \mu'_w = 1, \text{ all other } \mu = 1$$

$$P_d = \frac{20 \times 10 - 10 \times 10}{1 \times 1 \times 1} = 100$$

$$P_e = \frac{20 \times 10 - 10 \times 10}{1 \times 1} = 100$$

$$\lambda_{c\phi} = \frac{100 \tan(30)}{5} = 11.55$$

For $\lambda_{c\phi} = 11.55$ and $\beta = 35^\circ \rightarrow \cot\beta = 1.43 \rightarrow N_{cf} = 27$

$$F = \frac{27 \times 5}{100} = 1.35$$

For $\lambda_{c\phi} = 11.55$ and $\beta = 35^\circ \rightarrow \cot\beta = 1.43 \rightarrow x_o = 0$ and $y_o = 1.82$
Therefore, $X_o = 0$ and $Y_o = 18.2$ m.

b. Case 2: $H_w = 0$, $H'_w = 10$ m

$$\mu_w = \mu'_w = 1, \text{ all other } \mu = 1$$

$$P_d = \frac{20 \times 10}{1 \times 1 \times 1} = 200$$

$$P_e = \frac{20 \times 10 - 10 \times 10}{1 \times 1} = 100$$

$$\lambda_{c\phi} = \frac{100 \tan(30)}{5} = 11.55$$

For $\lambda_{c\phi} = 11.55$ and $\beta = 35^\circ \rightarrow \cot\beta = 1.43 \rightarrow N_{cf} = 27$

$$F = \frac{27 \times 5}{200} = 0.675$$

For $\lambda_{c\phi} = 11.55$ and $\beta = 35^\circ \rightarrow \cot\beta = 1.43 \rightarrow x_o = 0$ and $y_o = 1.82$
Therefore, $X_o = 0$ and $Y_o = 18.2$ m.

c. Case 3: $H_w = 0$, $H'_w = 0$

$$\mu_w = \mu'_w = 1, \text{ all other } \mu = 1$$

$$P_d = \frac{20 \times 10}{1 \times 1 \times 1} = 200$$

$$P_e = \frac{20 \times 10}{1 \times 1} = 200$$

$$\lambda_{c\phi} = \frac{200 \tan(30)}{5} = 23.1$$

For $\lambda_{c\phi} = 23.1$ and $\beta = 35^\circ \rightarrow \cot\beta = 1.43 \rightarrow N_{cf} = 47$

$$F = \frac{47 \times 5}{200} = 1.175$$

For $\lambda_{c\phi} = 23.1$ and $\beta = 35^\circ \rightarrow \cot\beta = 1.43 \rightarrow x_o = -0.2$ *and* $y_o = 2$
Therefore, $X_o = -2$ m and $Y_o = 20$ m.

Problem 19.6

A 3 horizontal to 1 vertical slope is cut in a clay that has an effective stress cohesion of 5 kPa and an effective stress friction angle of 30°. The slope is 6 m high. Calculate:

a. The factor of safety of the slope against long-term failure if the water table is below the critical circle.
b. The factor of safety of the slope against long-term failure if the water table coincides with the slope contour.

Solution 19.6

The slope angle is: $\tan\beta = \frac{1}{3}$ *then* $\beta = 18.42^\circ$

a. Dry Case, No Water

a-1. Taylor (1948)

Assume depth factor as D = 0.5, $\beta = 18.5^\circ$, $c' = 5$ kPa, $\varphi' = 30^\circ$, and $\gamma = 20$ kN/m^3.

$$F'_c = \frac{c'}{c'_d} \quad and \quad F'_\varphi = \frac{\tan\varphi'}{\tan\varphi'_d}$$

Iteration #1, FS = 1.5:

$$F'_c = \frac{c'}{c'_d} \rightarrow 1.5 = \frac{5}{c'_d} \rightarrow c'_d = 3.33 \text{ kPa}$$

The stability number $N = \frac{c'_d}{\gamma H} = \frac{3.33}{20\times 6} = 0.0277 \rightarrow$ Figure 19.13 $\rightarrow \varphi'_d = 11^\circ$

$$F'_\varphi = \frac{\tan\varphi'}{\tan\varphi'_d} = \frac{\tan 30}{\tan 11} = 2.97$$

Iteration #2, FS = 2.2:

$$F'_c = \frac{c'}{c'_d} \rightarrow 2.2 = \frac{5}{c'_d} \rightarrow c'_d = 2.27 \text{ kPa}$$

The stability number $N = \dfrac{c'_d}{\gamma H} = \dfrac{2.27}{20 \times 6} = 0.019 \rightarrow$ Figure 19.13 $\rightarrow \varphi'_d = 14.5^\circ$

$$F'_\varphi = \frac{\tan\varphi'}{\tan\varphi'_d} = \frac{\tan 30}{\tan 14.5} = 2.23$$

The safety factor would be 2.21.

a-2. Spencer (1967)

$$r_u = \frac{u_w}{\sigma_{0v}} \text{ assumed equal to } 0$$

Iteration #1, FS = 1.5:

$$F'_c = \frac{c'}{c'_d} \quad and \quad F_{\varphi'} = \frac{\tan\varphi'}{\tan\varphi'_d}$$

$$F'_c = \frac{c'}{c'_d} \rightarrow 1.5 = \frac{5}{c'_d} \rightarrow c'_d = 3.33 \text{ kPa} \quad \text{and} \quad N = \frac{c'_d}{\gamma H} = \frac{3.33}{20 \times 6} = 0.0277$$

Figure 19.15 $\rightarrow r_u = 0 \rightarrow \varphi'_d = 12^\circ$

$$F'_\varphi = \frac{\tan\varphi'}{\tan\varphi'_d} = \frac{\tan 30}{\tan 12} = 2.7$$

Iteration #2, FS = 2.5:

$$F'_c = \frac{c'}{c'_d} \rightarrow 2.5 = \frac{5}{c'_d} \rightarrow c'_d = 2 \text{ kPa}$$

The stability number $N = \dfrac{c'_d}{\gamma H} = \dfrac{2}{20 \times 6} = 0.017 \rightarrow$ Figure 19.15 $\rightarrow \varphi'_d = 14^\circ$ $F'_\varphi = \dfrac{\tan \varphi'}{\tan \varphi'_d} = \dfrac{\tan 30}{\tan 14} = 2.3$
The average safety factor would be 2.4.

b. Water Case, water level at ground surface

b-1. Spencer (1967), Drained behavior: c′, φ′

$$r_u = \frac{u_w}{\sigma_{0v}} = 0.5$$

Iteration #1, FS = 1.5:
Figure 19.15 $\rightarrow r_u = 0.5$, $N = \dfrac{c'_d}{\gamma H} = \dfrac{3.33}{20 \times 6} = 0.0277 \rightarrow \varphi'_d = 23^\circ$

$$F'_\varphi = \frac{\tan \varphi'}{\tan \varphi'_d} = \frac{\tan 30}{\tan 23} = 1.36$$

Factor of safety is about 1.43.

Problem 19.7

Calculate the probability of failure of a slope that has a factor of safety with a mean of 1.5 and a coefficient of variation of 0.2 (assume that the factor of safety is normally distributed). If the acceptable probability of failure is 0.001, what must be the mean value of the factor of safety if the coefficient of variation remains equal to 0.2?

Solution 19.7

Probability of Failure for a Given Factor of Safety

Mean, $\mu = 1.5$
Coefficient of variation, $CoV = 0.2$
Acceptable probability of failure, $\text{PoF}_{\text{ac}} = 0.001$
Standard deviation σ:
$CoV = \dfrac{\sigma}{\mu}$
$\sigma = \mu \cdot CoV = 1.5 \times 0.2 = 0.3$
Standard normal variable U of F = 1:

$$u = \frac{F - \mu_F}{\sigma_F} = \frac{1 - 1.5}{0.3} = -1.67$$

$$P(F < 1) = P\left(\frac{F - \mu_F}{\sigma_F} < \frac{1 - \mu_F}{\sigma_F}\right) = P(U < -1.67)$$

Using Table 11.3,

$$\text{P(U} < 1.67) = 0.9525$$

$$\text{P(U} < \text{u}) = 1 - \text{P(U} < -\text{u})$$

$$\text{P(U} < -1.67) = 1 - 0.9525 = 0.0475 \text{ or } 4.75\% \text{ probability of failure}$$

Factor of Safety for a Given Probability of Failure

$$P(F < 1) = 0.001$$

$$P(F < 1) = P\left(\frac{F - \mu_F}{\sigma_F} < \frac{1 - \mu_F}{\sigma_F}\right) = P\left(\frac{F - \mu_F}{0.2\mu_F} < \frac{1 - \mu_F}{0.2\mu_F}\right) = P\left(U < \frac{1 - \mu_F}{0.2\mu_F}\right) = 0.001$$

Using Table 11.3, we get:

$$P(U < 3.1) = 0.999 \quad or \quad P(U < -3.1) = 0.001$$

Therefore, we must have:

$$\frac{1-\mu_F}{0.2\mu_F} = -3.1 \quad or \quad \mu_F = 2.63$$

Problem 19.8

Which situation is more desirable? Explain and demonstrate.

a. Mean factor of safety F = 1.5 and coefficient of variation of F = 0.2
b. Mean factor of safety F = 1.3 and coefficient of variation of F = 0.1

Solution 19.8

$$CoV = \frac{\sigma}{\mu}$$

$$\sigma_a = CoV.\mu = 0.2 \times 1.5 = 0.3$$

$$\sigma_b = CoV.\mu = 0.1 \times 1.3 = 0.13$$

$$P(F<1) = P\left(\frac{F-\mu_F}{\sigma_F} < \frac{1-\mu_F}{\sigma_F}\right) = P\left(\frac{F-1.5}{0.3} < \frac{1-1.5}{0.3}\right)$$

$$= P(U<-1.67) = 1 - P(U<1.67) = 1 - 0.9525 = 0.0475$$

$$P(F<1) = P\left(\frac{F-\mu_F}{\sigma_F} < \frac{1-\mu_F}{\sigma_F}\right) = P\left(\frac{F-1.3}{0.13} < \frac{1-1.3}{0.13}\right)$$

$$= P(U<-2.31) = 1 - P(U<2.31) = 1 - 0.9896 = 0.0104$$

Therefore, a mean factor of safety of 1.3 with a coefficient of variation of 0.1 (case b) is more desirable than a mean factor of safety of 1.5 and a coefficient of variation of 0.2 (case a). The reason is that the probability of failure is 1.04% in case b and 4.75% in case a.

Problem 19.9

Calculate the factor of safety for the slope shown in Figure 19.3s. Select your best estimate of the critical circle and calculate the factor of safety by the Bishop modified method of slices.

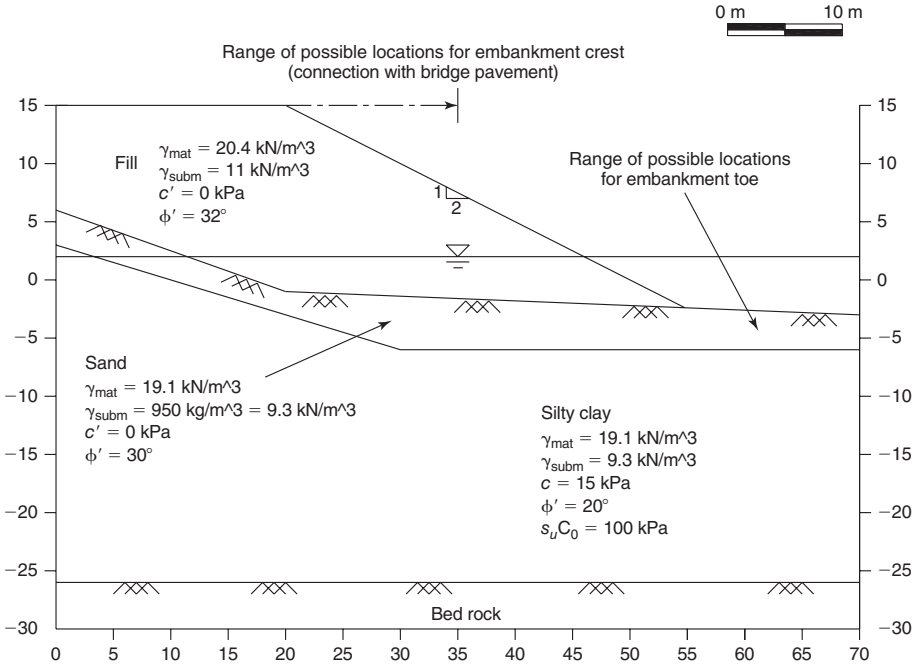

Figure 19.3s Slope of Fredericton embankment.

Solution 19.9

The sketch for the simplified method of slices is shown in Figure 19.6s. The results are shown in Table 19.2s.

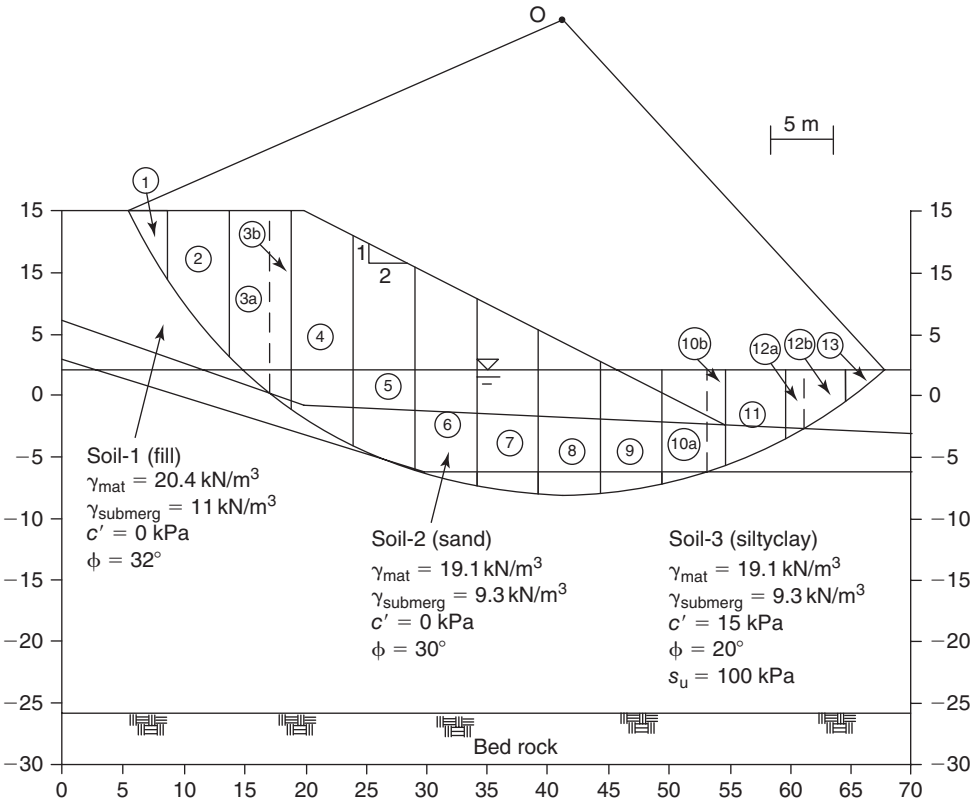

Figure 19.6s Bishop Simplified Method of Slices.

Problem 19.10

A slope is subjected to an acceleration history as shown in Figure 19.4s. The yield acceleration for that slope is 1.5 m/s^2. Calculate the displacement history of the slope according to Newmark's method.

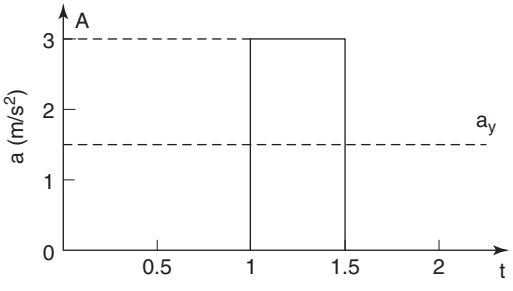

Figure 19.4s Acceleration history.

Table 19.2s Summary of the Results of the Bishop Simplified Method of Slices

Slice #	φ′	b (m)	Area fill ($m2^2$)		Area total (m^2)	Unit Weight (kN/m^3)	Weight (kN/m)	Total Weight (kN/m)	θ	$\cos\theta_i$	Wsinθ (kN)	b (m)	hp (m)	u_w (kPa)	$u_w b_i$ (kN/m)	$(W-u_w b)\tan\varphi'$ (kN)	c′ (kN/m)	c′b/cosθ (kN/m)	m_θ	$[cb+(W-u_w b)\tan\varphi']/m_\theta$
1	32	3.2	Soil-1 (100%)	9.0	9.0	20.40	183.6	183.6	60.0	0.50	159.00	3.20	0.00	0.00	0.00	114.73	0.00	0.00	0.87	131.38
2	32	5.0	Soil-1 (100%)	43.5	43.5	20.40	887.4	887.4	51.1	0.63	690.61	5.00	0.00	0.00	0.00	554.51	0.00	0.00	0.96	575.61
3a	32	3.3	Soil-1 (95%)	66.3	66.3	20.40	1352.5	1352.5	42.7	0.73	917.22	3.25	0.90	8.83	28.69	827.22	0.00	0.00	1.03	805.34
3b	30	1.8	Soil-2 (5%)	3.5	3.5	19.10	66.9	66.9	36.6	0.80	39.86	1.75	2.60	25.51	44.64	12.83	0.00	0.00	1.04	12.33
4	30	5.0	Soil-1 (90%)	8.0	82.8	20.40	163.2	1591.9	30.1	0.87	798.34	5.00	5.00	49.05	245.25	777.48	0.00	0.00	1.06	730.14
			Soil-2 (10%)	74.8		19.10	1428.7													
5	30	5.0	Soil-1 (60%)	26.6	44.4	20.40	543.5	882.7	21.8	0.93	327.80	5.00	7.22	70.83	354.14	305.15	0.00	0.00	1.08	283.50
			Soil-2 (40%)	17.8		19.10	339.2													
6	20	5.0	Soil-1 (68%)	51.7	76.0	20.40	1054.7	1518.8	11.9	0.98	313.18	5.00	8.90	87.31	436.55	393.91	15.00	75.00	1.03	455.14
			Soil-2 (28%)	21.3		19.10	406.8													
			Soil-3 (4%)	3.0		19.10	57.3													
7	20	5.0	Soil-1 (57%)	40.6	71.2	20.40	828.2	1411.7	7.3	0.99	179.38	5.00	9.80	96.14	480.69	338.88	15.00	75.00	1.02	404.26
			Soil-2 (33%)	23.3		19.10	445.0													
			Soil-3 (10%)	7.3		19.10	138.5													
8	20	5.0	Soil-1 (49%)	29.1	59.8	20.40	593.6	1180.0	0.0	1.00	0.00	5.00	10.14	99.47	497.37	248.46	15.00	75.00	1.00	323.46
			Soil-2 (36%)	22.0		19.10	420.2													
			Soil-3 (15%)	8.7		19.10	166.2													
9	20	5.0	Soil-1 (36%)	17.5	48.7	20.40	357.0	920.4	-9.1	0.99	-145.57	5.00	9.70	95.16	475.79	161.83	15.00	75.00	0.95	249.89
			Soil-2 (43%)	20.9		19.10	399.2													
			Soil-3 (14%)	6.8		19.10	129.9													
			Water (7%)	3.5		9.81	34.3													
10a	20	3.5	Soil-1 (18%)	5.4	29.8	20.40	110.8	486.8	-15.1	0.97	-126.81	3.50	8.90	87.31	305.58	65.96	15.00	52.50	0.90	131.61
			Soil-2 (44%)	13.1		19.10	250.2													
			Soil-3 (5%)	1.6		19.10	30.6													
			Water (33%)	9.7		9.81	95.3													
10b	30	1.5	Soil-1 (5%)	0.5	11.8	20.40	10.8	167.7	-20.1	0.94	-57.63	1.50	8.00	78.48	117.72	28.86	0.00	0.00	0.80	35.97
			Soil-2 (43%)	5.0		19.10	96.1													
			Water (53%)	6.2		9.81	60.8													
11	30	5.0	Soil-2 (32%)	10.5	33.5	19.10	200.6	426.2	-23.7	0.92	-171.30	5.00	6.70	65.73	328.64	56.32	0.00	0.00	0.76	74.53
			Water (68%)	23.0		9.81	225.6													
12a	30	5.0	Soil-2 (17%)	0.7	4.2	19.10	13.4	48.0	-31.2	0.86	-24.86	5.00	5.23	51.31	256.53	0.00	0.00	0.00	0.65	0.00
			Water (83%)	3.5		9.81	34.6													
12b	0	3.5	Water (100%)	12.7	12.7	9.81	124.6	124.6	-60.0	0.50	-107.90	3.50	3.86	37.87	132.53	0.00	0.00	0.00	0.50	0.00
13	0	3.2	Water (100%)	4.1	4.1	9.81	40.2	40.2	-68.0	0.37	-37.29	3.20	1.50	14.72	47.09	0.00	0.00	0.00	0.37	0.00
										Σ	**2754.0**						**Σ**	**352.50**		**4213.17**
Note: the percentage number in the section of the area stand for the corresponding area for each of the slide in consideration.																			**F.S.=**	**1.53**

Solution 19.10

From Figure 19.4s: single rectangular acceleration, $A = 3\ \text{m/s}^2$, yield acceleration, $a_y = 1.5\ \text{m/s}^2$, relative acceleration $a_{rel}(t)$, relative velocity $v_{rel}(t)$ and relative displacement $d_{rel}(t)$.

At $t_0 \le t \le t_0 + \Delta t$ or $1 < \text{t} < 1.5$ seconds, relative acceleration, relative velocity, and relative displacement are:

$$a_{rel}(t) = A - a_y = 3 - 1.5 = 1.5\ \text{m/s}^2$$

$$v_{rel}(t) = \int_{t_0}^{t} a_{rel}(t)dt = [A - a_y](t - t_0) = [3 - 1.5](t - 1) = 1.5t - 1.5\ \text{m/s}$$

$$d_{rel}(t) = \int_{t_0}^{t} v_{rel}(t)dt = \frac{1}{2}[A - a_y](t - t_0)^2 = \frac{1}{2}[3 - 1.5](t - 1)^2 = 0.75(t - 1)^2\ \text{m}$$

At $t_0 = t_0 + \Delta t$ or 1.5 seconds:

$$v_{rel}(t + \Delta t) = [A - a_y]\Delta t = [3 - 1.5] \times 0.5 = 0.75\ \text{m/s}$$

$$d_{rel}(t + \Delta t) = \frac{1}{2}[A - a_y]\Delta t^2 = \frac{1}{2}[3 - 1.5]0.5^2 = 0.1875\ \text{m}$$

At $t_0 + \Delta t \le t \le t_1$ or $1.5 < \text{t} < 2$ seconds:

$$a_{rel}(t) = 0 - a_y = -1.5\ \text{m/s}^2$$

$$v_{rel}(t) = 0.75 + \int_{1.5}^{t} a_{rel}(t)dt = 0.75 + \int_{1.5}^{t} (-1.5)dt = -1.5t + 3\ \text{m/s}$$

$$d_{rel}(t) = 0.1875 + \int_{1.5}^{t} v_{rel}(t)dt = 0.1875 + \int_{1.5}^{t} (-1.5t + 3)dt = -0.75t^2 + 3t - 2.625$$

All results are plotted in Figure 19.7s.

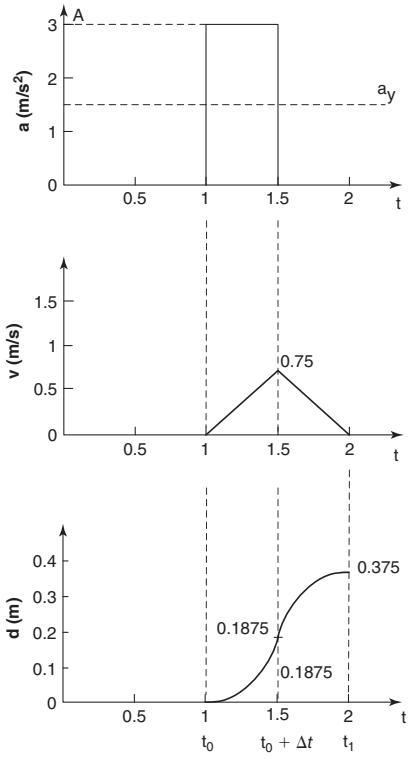

Figure 19.7s Acceleration, velocity, and displacement history of a slope.

Problem 19.11

Consider the case of a $c' = 0$, $\varphi' > 0$ soil and demonstrate that for one slice, the factor of safety is the same for the ordinary method of slices (OMS) and for the Bishop simplified method of slices (BSMS). If it is true for one slice, why is it not true for n slices ($n > 1$)?

Solution 19.11

OMS

$$F = \frac{W \cos\theta \tan\varphi}{W \sin\theta} = \frac{\tan\varphi}{\tan\theta}$$

BSMS

$$m = \cos\theta \left(1 + \frac{\tan\theta \tan\varphi}{F}\right)$$

$$F = \frac{\frac{1}{m}(W \tan\varphi)}{W \sin\theta} = \frac{\tan\varphi}{\cos\theta \sin\theta \left(1 + \frac{\tan\theta \tan\varphi}{F}\right)}$$

$$\frac{\tan\varphi}{F} = \cos\theta \sin\theta \left(1 + \frac{\tan\theta \tan\varphi}{F}\right)$$

$$\frac{\tan\varphi}{F}(1 - \cos\theta \sin\theta \tan\theta) = \cos\theta \sin\theta$$

$$F = \frac{\tan\varphi(1 - \sin^2\theta)}{\cos\theta \sin\theta} = \frac{\tan\varphi \cos^2\theta}{\cos\theta \sin\theta} = \frac{\tan\varphi}{\tan\theta}$$

The assumption in both methods is with respect to side forces. Because we have only one slice, there are no side forces between slices. Most importantly, there are as many unknowns as there are equations, so equilibrium equations can be written in any direction and will lead to the same answer. The three unknowns are S_m, N', and F; the three equations are vertical equilibrium, horizontal equilibrium, and the shear strength equation. Moment equilibrium is automatically satisfied because all forces go through the middle of the base of the slice. Thus, both methods should give identical safety factor. This is no longer true when we have more than one slice, because the assumptions are different for the side forces.

Problem 19.12

A 3D slope failure has a failure surface in the form of a sphere and a factor of safety F_{3D}. This sphere is sliced in a direction perpendicular to the crest. The slices have the same width b. The deepest slice in the center of the sphere has a factor of safety F_{min}. Each slice has a 2D factor of safety equal to F_i. What other assumptions must be made for the following equation to be true?

$$F_{3D} = \frac{1}{n}\sum_{i=1}^{n} F_i$$

Solution 19.12

As explained in section 19.16, in order to use this equation for the safety factor F_{3D}:

1. The axis of rotation must be the same for all slices (Figure 19.34)
2. The forces between circle slices must be negligible

Problem 19.13

A dry, fine sand slope has a factor of safety of 1.5 on the Earth.

a. Calculate and discuss the factor of safety for the same slope on the moon.
b. Assume that there could be water on the moon. Would the result of the dry case still hold?

Solution 19.13

a. The factor of safety for dry sand is $F = \dfrac{\tan\varphi'}{\tan\beta}$. It is independent of gravity acceleration (g), so it would be the same on the moon.
b. It would be if the water was at the surface of the slope, but it would not be if the slope was above the groundwater level and water tension developed in the slope. Because water tension is a chemically-based phenomenon and not a gravity-based phenomenon, it would be the same on the Earth and on the moon, but its ratio to gravity forces would be very different. Therefore, it would lead to different factors of safety. The same slope would be safer on the moon if water tension existed in both cases.

Problem 19.14

Define the seepage force and discuss when the seepage force should be considered in a slope stability analysis. Why is it not usually considered?

Solution 19.14

The seepage force is the force exerted in friction by water flowing around soil particles and trying to drag them away. The forces shown on a free-body diagram are the external forces. The internal forces are resolved internally. The seepage force is an external force when the soil skeleton is considered as the free body, but it is an internal force when the soil skeleton plus the water is considered as the free body. Most slope stability analyses consider the soil skeleton plus the water as the free body. In those instances, the seepage force must not be included in any slope stability calculations.

Problem 19.15

Explain the difference between the following analyses, including what shear strength you would use: total stress analysis, effective stress analysis, undrained analysis, drained analysis, short-term analysis, long-term analysis.

Solution 19.15

A total stress analysis considers that the soil is made of one material. During the analysis, the three components (particles, water, and air) are not recognized. This analysis can be used in the case of a soil with no water and in the case of a soil where the shear strength is independent of rapid variations in total stress.

An effective analysis can be used in all cases. It makes no particular assumption regarding drainage and is based on sound fundamental principles. It makes use of the effective stress equation to obtain the shear strength of the soil based on effective stress cohesion c′ and the effective stress friction angle φ' ($\tau = c' + \sigma' \tan\varphi'$). It can be used for an undrained analysis, a drained analysis, a short-term analysis, or a long-term analysis. The difficulty with this method is that the water stress in the mass must be known.

An undrained analysis is used in the case where the water is not allowed or does not have time to drain away. The soil strength parameter used in this case is the undrained shear strength (s_u).

In a drained analysis, the water stress is considered to be hydrostatic throughout the mass. The soil strength parameters used are the drained strength parameters or effective stress parameters ($\tau = c' + \sigma' \tan\varphi'$).

A short-term analysis considers a time shortly after loading. It is often a drained analysis for fast-draining soils like free-draining sands and gravels, and an undrained analysis for slow-draining soils like silts and clays. In the case of free-draining sands and gravels, the drained strength parameters are used. In the case of silts and clays, the undrained shear strength (s_u) is used.

A long-term analysis considers that all water stresses induced by loading have had time to dissipate and are back to hydrostatic condition. In this regard a long-term analysis is similar to a drained analysis. The soil strength parameters used are the drained strength parameters or effective stress parameters ($\tau = c' + \sigma' \tan\varphi'$).

Problem 19.16

An inclinometer casing is attached to a 10 m high retaining wall. Zero readings taken before the wall is backfilled indicate that the wall is perfectly vertical. The backfill is placed and compacted. At the end of construction, the inclinometer readings are taken again. Find what the readings are if:

a. The displacement y (m) of the wall obeys the equation $y = 0.01\ (z_{max} - z)$ where z_{max} is the maximum depth the inclinometer probe can reach in the casing (10 m) and z is the depth at which the reading is taken.

b. The displacement y (m) of the wall obeys the equation $y = 0.001\ (z_{max} - z)^2$ where z_{max} is the maximum depth the inclinometer probe can reach in the casing (10 m) and z is the depth at which the reading is taken.

The inclinometer has a calibration constant C = 20,000 and a wheel spacing of 0.5 m.

Solution 19.16

Assume that the constant parameter for the inclinometer is C = 20,000, and the length of probe between wheels is L = 0.5 m. Figure 19.8s shows the wall and inclinometer.

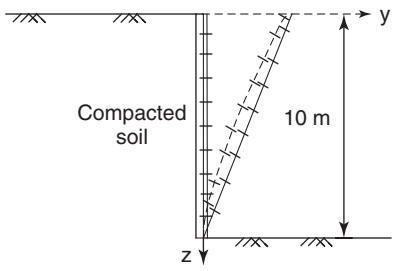

Figure 19.8s Illustration of the inclinometer.

The equation for the displacement D_n of the inclinometer casing is:

$$D_n = \sum_{i=1}^{n}(d_i - d_{io}) = \frac{L}{C}\sum_{i=1}^{n}(R_i - R_{io})$$

where D_n is the displacement at a depth z_n from the surface, z_n is the depth to the first (deepest) reading in the casing minus n times the distance L between readings, d_i is the difference in horizontal displacement between the i and $i-1$ reading points, d_{io} is the initial value of d_i, L is the length between readings, C is the inclinometer calibration constant, R_i is the reading at depth z_i, and R_{io} is the initial value of R_i.

Case a. In this case the wall deforms by simple rotation and the displacement y(m) of the wall is linear. The equation for D_n becomes:

$$D_n = \sum_{i=1}^{n} d_i = \frac{L}{C}\sum_{i=1}^{n} R_i$$

But D_n is also given in the problem as:

$$D_n = 0.01(10 - z)$$

Therefore, the difference between two consecutive readings is:

$$D_n - D_{n-1} = d_n = 0.01(10 - z) - 0.01(10 - z - 0.5) = 0.005 \text{ m}$$

The increment of displacement is constant and the angle of the wall is also constant:

$$\theta_n = \sin^{-1}\frac{d_n}{L} = \sin^{-1}\frac{0.005}{0.5} \simeq 0.01 \text{ rd}$$

Furthermore, D_o is equal to zero, because the bottom of the wall does not move. Now the reading is equal to:

$$R_n = \frac{C}{L}d_n = \frac{20000}{0.5} \times 0.005 = 200$$

So the reading of the inclinometer is constant equal to 200; Table 19.3s summarizes the results.

Case b. In this case, the displacement y(m) of the wall is nonlinear. The equation for D_n is still:

$$D_n = \sum_{i=1}^{n} d_i = \frac{L}{C}\sum_{i=1}^{n} R_i$$

But D_n is also given in the problem as:

$$D_n = 0.001(10 - z)^2$$

Therefore, the difference between two consecutive readings is:

$$D_n - D_{n-1} = d_n = 0.001(10 - z)^2 - 0.001(10 - z - 0.5)^2 = 0.001(9.75 - z)$$

The increment of displacement increases linearly with z and so does the angle of the wall:

$$\theta_n = \sin^{-1}\frac{0.001(9.75 - z)}{L} = \sin^{-1}\frac{d_n}{L}$$

Furthermore, D_o is equal to zero, because the bottom of the wall does not move. Now the reading is equal to:

$$R_n = \frac{C}{L}d_n = \frac{20000}{0.5} \times 0.001(9.75 - z) = 390 - 40z$$

Table 19.4s summarizes the results.

Table 19.3s Inclinometer Readings for Linear Displacement of Wall

Depth z (m)	Displacement y (m)	Inclined angle (radians)	Inclined angle (degree)	Inclinometer reading (R)
10	0	0.009999667	0.572938698	0
9.5	0.005	0.009999667	0.572938698	200
9	0.01	0.009999667	0.572938698	200
8.5	0.015	0.009999667	0.572938698	200
8	0.02	0.009999667	0.572938698	200
7.5	0.025	0.009999667	0.572938698	200
7	0.03	0.009999667	0.572938698	200
6.5	0.035	0.009999667	0.572938698	200
6	0.04	0.009999667	0.572938698	200
5.5	0.045	0.009999667	0.572938698	200
5	0.05	0.009999667	0.572938698	200
4.5	0.055	0.009999667	0.572938698	200
4	0.06	0.009999667	0.572938698	200
3.5	0.065	0.009999667	0.572938698	200
3	0.07	0.009999667	0.572938698	200
2.5	0.075	0.009999667	0.572938698	200
2	0.08	0.009999667	0.572938698	200
1.5	0.085	0.009999667	0.572938698	200
1	0.09	0.009999667	0.572938698	200
0.5	0.095	0.009999667	0.572938698	200
0	0.1	0.009999667	0.572938698	200

Table 19.4s Inclinometer Readings for Linear Displacement of Wall

Depth z (m)	Displacement y (m)	Inclined angle (radians)	Inclined angle (degree)	Inclinometer reading (R)
10	0	0	0	0
9.5	0.00025	0.0005	0.028648	10
9	0.001	0.0014997	0.085943	30
8.5	0.00225	0.0024995	0.143239	50
8	0.004	0.0034993	0.200535	70
7.5	0.00625	0.0044992	0.257832	90
7	0.009	0.0054990	0.315128	110
6.5	0.01225	0.0064988	0.372425	130
6	0.016	0.0074986	0.429722	150
5.5	0.02025	0.0084985	0.487020	170
5	0.025	0.0094983	0.544318	190
4.5	0.03025	0.0104982	0.601617	210
4	0.036	0.0114981	0.658916	230
3.5	0.04225	0.0124980	0.716216	250
3	0.049	0.0134978	0.773516	270
2.5	0.05625	0.0144978	0.830818	290
2	0.064	0.0154977	0.888120	310
1.5	0.07225	0.0164976	0.945423	330
1	0.081	0.0174976	1.002727	350
0.5	0.09025	0.0184976	1.060032	370
0	0.1	0.0194975	1.117338	390